5. Green S, Chambon P 1988 Nuclear receptors enhance our understanding of transcription regulation. Trends Genet 4:309–314
6. Glass CK, Rosenfeld MG 2000 The coregulator exchange in transcriptional functions of nuclear receptors. Genes Dev 14:121–141
7. Williams DL, Sensel M, McTigue M, Binder R 1993 Hormonal and developmental regulation of mRNA turnover. In: Belasco J, Brawerman G, eds. Control of messenger RNA stability. New York: Academic Press; 161–197
8. Chen CY, Shyu AB 1995 AU-rich elements: characterization and importance in mRNA degradation. Trends Biochem Sci 20:465–470
9. Myer VE, Fan XC, Steitz JA 1997 Identification of HuR as a protein implicated in AUUUA-mediated mRNA decay. EMBO J 16:2130–2139
10. Lai WS, Carballo E, Strum JR, Kennington EA, Phillips RS, Blackshear PJ 1999 Evidence that tristetraprolin binds to AU-rich elements and promotes the deadenylation and destabilization of tumor necrosis factor α mRNA. Mol Cell Biol 19:4311–4323
11. Brewer G 1991 An A+U-rich element RNA-binding factor regulates c-myc mRNA stability in vitro. Mol Cell Biol 11:2460–2466
12. Kiledjian M, DeMaria C, Brewer G, Novick K 1997 Identification of AUF1 (heterogeneous nuclear ribonucleoprotein D) as a component of the α-globin mRNA stability complexes. Mol Cell Biol 17:4870–4876
13. Pende A, Tremmel KD, DeMaria CT, Blaxall BC, Minobe WA, Sherman JA, Bisognano JD, Bristow MR, Brewer G, Port JD 1996 Regulation of the mRNA-binding protein AUF1 by activation of the β-adrenergic receptor signal transduction pathway. J Biol Chem 271:8493–8501
14. Sirenko OI, Lofquist AK, DeMaria CT, Morris JS, Brewer G, Haskill JS 1997 Adhesion-dependent regulation of an A+U-rich element-binding activity associated with AUF1. Mol Cell Biol 17:3894–3906
15. Sela-Brown A, Silver J, Brewer G, Naveh-Many T 2000 Identification of AUF1 as a parathyroid hormone mRNA 3′-untranslated region-binding protein that determines parathyroid hormone mRNA stability. J Biol Chem 275: 7424–7429
16. Chen CY, Gherzi R, Ong SE, Chan EL, Raijmakers R, Pruijn GJ, Stoecklin G, Moroni C, Mann M, Karin M 2001 AU binding proteins recruit the exosome to degrade ARE-containing mRNAs. Cell 107:451–464
17. Dempsey LA, Li M, Depace A, Bray-Ward P, Maizels N 1998 The human HNRPD locus maps to 4q21 and encodes a highly conserved protein. Genomics 49:378–384
18. Wagner BJ, DeMaria CT, Sun Y, Wilson GM, Brewer G 1998 Structure and genomic organization of the human AUF1 gene: alternative pre-mRNA splicing generates four protein isoforms. Genomics 48:195–202
19. Arao Y, Kikuchi A, Ikeda K, Nomoto S, Horiguchi H, Kayama F 2002 A+U-rich-element RNA-binding factor 1/heterogeneous nuclear ribonucleoprotein D gene expression is regulated by oestrogen in the rat uterus. Biochem J 361:125–132
20. Arao Y, Kuriyama R, Kayama F, Kato S 2000 A nuclear matrix-associated factor, SAF-B interacts with specific isoforms of AUF1/hnRNP D. Arch Biochem Biophys 380: 228–236
21. VanHuffel S, Delaei F, Heyninck K, DeValck D, Beyaert R 2001 Identification of a novel a20-binding inhibitor of nuclear factor-κB activation termed ABIN-2. J Biol Chem 276:30216–30223
22. Charles CH, Simske JS, O'Brien TP, Lau LF 1990 Pip92: a short-lived, growth factor-inducible protein in BALB/c 3T3 and PC12 cells. Mol Cell Biol 10:6769–6774
23. Coleclough C, Kuhn L, Lefkovits I 1990 Regulation of mRNA abundance in activated T lymphocytes: identification of mRNA species affected by the inhibition of protein synthesis. Proc Natl Acad Sci USA 87:1753–1757
24. DeMaria CT, Sun Y, Long L, Wagner BJ, Brewer G 1997 Structural determinants in AUF1 required for high affinity binding to A + U-rich elements. J Biol Chem 272: 27635–27643
25. Rhee Y, Gurel F, Gafni Y, Dingwall C, Citovsky V 2000 A genetic system for detection of protein nuclear import and export. Nat Biotechnol 18:433–437
26. Sarkar B, Lu JY, Schneider RJ 2003 Nuclear import and export functions in the different isoforms of the AUF1/heterogeneous nuclear ribonucleoprotein protein family. J Biol Chem 278:20700–20707
27. Hughes DP, Marron MB, Brindle NP 2003 The antiinflammatory endothelial tyrosine kinase Tie2 interacts with a novel nuclear factor-κB inhibitor ABIN-2. Circ Res 92: 630–636
28. Tadros A, Hughes DP, Dunmore BJ, Brindle NP 2003 ABIN-2 protects endothelial cells from death and has a role in the antiapoptotic effect of angiopoietin-1. Blood 102:4407–4409
29. Wong AL, Haroon ZA, Werner S, Dewhirst MW, Greenberg CS, Peters KG 1997 Tie2 expression and phosphorylation in angiogenic and quiescent adult tissues. Circ Res 81:567–574
30. Latinkic BV, Lau LF 1994 Transcriptional activation of the immediate early gene pip92 by serum growth factors requires both Ets and CArG-like elements. J Biol Chem 269:23163–23170
31. Chung KC, Gomes I, Wang D, Lau LF, Rosner MR 1998 Raf and fibroblast growth factor phosphorylate Elk1 and activate the serum response element of the immediate early gene pip92 by mitogen-activated protein kinase-independent as well as -dependent signaling pathways. Mol Cell Biol 18:2272–2281
32. Laroia G, Schneider RJ 2002 Alternate exon insertion controls selective ubiquitination and degradation of different AUF1 protein isoforms. Nucleic Acids Res 30: 3052–3058
33. Loflin P, Chan C-YA, Shyu AB 1999 Unraveling a cytoplasmic role for hnRNP D in the in vivo mRNA destabilization directed by the AU-rich element. Genes Dev 13: 1884–1897
34. Shyu A-B, Wilkinson MF 2000 The double lives of shuttling mRNA binding proteins. Cell 102:135–138
35. Fan XC, Steitz JA 1998 Overexpression of HuR, a nuclear-cytoplasmic shuttling protein, increases the in vivo stability of ARE-containing mRNAs. EMBO J 17: 3448–3460
36. Dean JL, Wait R, Mahtani KR, Sully G, Clark AR, Saklatvala J 2001 The 3′ untranslated region of tumor necrosis factor α mRNA is a target of the mRNA-stabilizing factor HuR. Mol Cell Biol 21:721–730
37. Yaman I, Fernandez J, Sarkar B, Schneider RJ, Snider MD, Nagy LE, Hatzoglou M 2002 Nutritional control of mRNA stability is mediated by a conserved AU-rich element that binds the cytoplasmic shuttling protein HuR. J Biol Chem 277:41539–41546
38. Bakheet T, Frevel M, Williams BR, Greer W, Khabar KS 2001 ARED: human AU-rich element-containing mRNA database reveals an unexpectedly diverse functional repertoire of encoded proteins. Nucleic Acids Res 29: 246–254
39. Liu J, Shen X, Nguyen VA, Kunos G, Gao B 2000 α_1 Adrenergic agonist induction of p21(waf1/cip1) mRNA stability in transfected HepG2 cells correlates with the increased binding of an AU-rich element binding factor. J Biol Chem 275:11846–11851
40. Giles KM, Daly JM, Beveridge DJ, Thomson AM, Voon DC, Furneaux HM, Jazayeri JA, Leedman PJ 2003 The 3′-untranslated region of p21WAF1 mRNA is a composite cis-acting sequence bound by RNA-binding proteins from breast cancer cells, including HuR and poly(C)-binding protein. J Biol Chem 278:2937–2946

41. Mahtani KR, Brook M, Dean JL, Sully G, Saklatvala J, Clark AR 2001 Mitogen-activated protein kinase p38 controls the expression and posttranslational modification of tristetraprolin, a regulator of tumor necrosis factor α mRNA stability. Mol Cell Biol 21:6461–6469
42. Johnson BA, Stehn JR, Yaffe MB, Blackwell TK 2002 Cytoplasmic localization of tristetraprolin involves 14–3-3-dependent and -independent mechanisms. J Biol Chem 277:18029–18036
43. Wang W, Fan J, Yang X, Furer-Galban S, Lopez de Silanes I, von Kobbe C, Guo J, Georas SN, Foufelle F, Hardie DG, Carling D, Gorospe M 2002 AMP-activated kinase regulates cytoplasmic HuR. Mol Cell Biol 22: 3425–3436
44. Wilson GM, Lu J, Sutphen K, Suarez Y, Sinha S, Brewer B, Villanueva-Feliciano EC, Ysla RM, Charles S, Brewer G 2003 Phosphorylation of p40AUF1 regulates binding to A+U-rich mRNA-destabilizing elements and protein-induced changes in ribonucleoprotein structure. J Biol Chem 278:33039–33048
45. Simoncini T, Hafezi-Moghadam A, Brazil DP, Ley K, Chin WW, Liao JK 2000 Interaction of oestrogen receptor with the regulatory subunit of phosphatidylinositol-3-OH kinase. Nature 407:538–541
46. Kousteni S, Bellido T, Plotkin LI, O'Brien CA, Bodenner DL, Han L, Han K, DiGregorio GB, Katzenellenbogen JA, Katzenellenbogen BS, Roberson PK, Weinstein RS, Jilka RL, Manolagas SC 2001 Nongenotropic, sex-nonspecific signaling through the estrogen or androgen receptors: dissociation from transcriptional activity. Cell 104: 719–730
47. Wilson GM, Lu J, Sutphen K, Sun Y, Huynh Y, Brewer G 2003 Regulation of A+U-rich element-directed mRNA turnover involving reversible phosphorylation of AUF1. J Biol Chem 278:33029–33038
48. Arao Y, Yamamoto E, Miyatake N, Ninomiya Y, Umehara T, Kawashima H, Masushige S, Hasegawa T, Kato S 1996 A synthetic estrogen antagonist inhibits estrogen-induced transcriptional, but not post-transcriptional regulation of gene expression. Biochem J 313:269–274

Molecular Endocrinology **is published monthly by The Endocrine Society (http://www.endo-society.org), the foremost professional society serving the endocrine community.**

CHAPTER 16

RING Finger-B Box-Coiled Coil (RBCC) Proteins as Ubiquitin Ligase in the Control of Protein Degradation and Gene Regulation

Kazuhiro Ikeda, Satoshi Inoue, Masami Muramatsu

Abstract

The protein family harboring the RING finger motif, de fined as a linear array of conserved cysteines and histidines, has grown enormously in the last decade. The members of the family are involved in various biological processes including growth, differentiation, apoptosis, transcription and also in diseases and oncogenesis. It has been postulated that the RING finger domains have crucial roles in these phenomena themselves, in some cases, working with other domains in other proteins, although the precise mechanisms and common features of RING finger function have not been fully elucidated. However, most recently, an accumulating body of evidence has revealed that some of the RING finger proteins work as E3 ubiquitin ligases in ubiquitin-mediated specific protein degradation pathway. In this review, we focus on the RING finger protein with special reference to E3 ligase.

Structure of RING Finger

The RING finger protein sequence motif was first identified in the human gene RING1 – Really Interesting New Gene 1 – which is located proximal to the major histocompatibility region on chromosome 6.[1,2] The RING finger motif can be defined as a unique linear series of conserved cysteine and histidine residues: Cys-X_2-Cys-X_{11-16}-Cys-X-His-X_2-Cys-X_2-Cys-X_{7-74}-Cys-X_2-Cys (RING-CH or C_3HC_4 type), where X can be any amino acid (Fig. 1). So far, three-dimensional structures of RING domains from human PML (for promyelocytic leukemia protein),[3] immediate early equine herpes virus (IEEHV) protein,[4] human recombination-activating gene 1 protein (RAG1),[5] human MAT1 (for menage a trois-1 protein)[6] and human Cbl (for Casitas B-lineage lymphoma protein)[7] with a cognate ubiquitin-conjugating enzyme (E2) have been solved at atomic resolution. These studies have confirmed that the RING finger binds zinc ions in a similar manner as the classical zinc finger motif. Particularly, the RING finger is composed of a unique 'cross-brace' arrangement with two zinc ions and folds into a compact domain comprising a small central β sheet and an α helix. There are subfamilies of RING fingers which have Cys5 substituted with histidine (RING-H2) and a cysteine or histidine substituted with other metal binding residues such as aspartic acid and threonine.[8,9] Although the RING domain was initially found

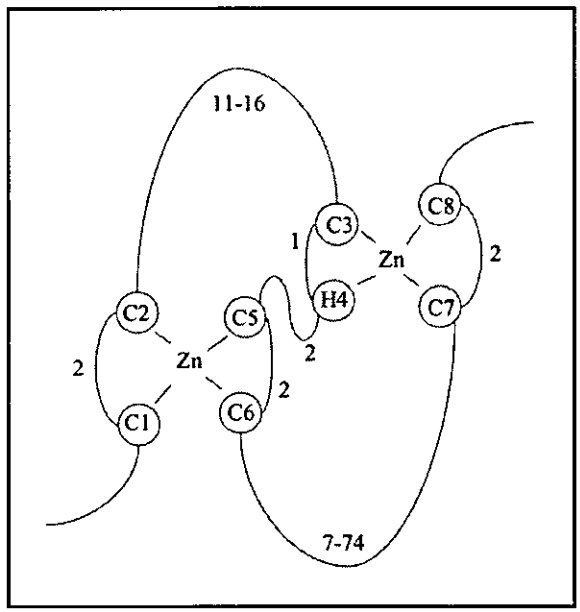

Figure 1. Schematic representation of the structure of RING finger domain. The metal-ligand residues, either cysteine (C) or histidine (H), are shown as numbered spheres. The numbers next to the loops connecting the metal-ligand residues indicate the minimum and maximum number of loop residues.

in only a few genes, more than 3000 proteins harboring the RING finger domain have been detected from diverse eukaryotes in the SMART database as of July 2003. Because of this evolutional conservation and variation in loop lengths, the RING domain appears to have a considerable flexibility within the rigid structure.

Family of RING Finger Protein

The RING fingers and their variants are generally located close to an amino or carboxyl terminus though there are no fixed rules. Most of the RING finger is associated with certain protein domains to form larger conserved motifs which may define the func-

Zinc Finger Proteins: From Atomic Contact to Cellular Function, edited by Shiro Iuchi and Natalie Kuldell.

tion of the protein, thus the family being divided into subfamilies along with the associated domains (Fig. 2). A similar domain architecture often corresponds with a similar function. For instance, TRAFs (for tumor necrosis factor (TNF) receptor-associated factors) 2-5 have an N-terminal RING domain followed by five zinc fingers, a coiled coil, and a C-terminal TRAF domain.[10] TRAF1 has all of these domains except for the RING. Members of TRAF family have been shown to be involved in TNF-related cytokine signal transduction through interactions between their TRAF domains and the intracytoplasmic parts of receptors of the TNF receptor family which are suicide receptors to transfer apoptotic signals into the cells.[11-13]

The inhibitors of apoptosis gene family, IAP1, IAP2 and XIAP, have a RING domain at their C termini and BIR (baculovirus IAP repeat) domain at their N termini. The BIR domains of the proteins bind and inhibit caspase.[14,15] Interestingly, the RING fingers of XIAP and IAP2 possess E3 ubiquitin ligase activity and are thought to be responsible for self-degradation when an apoptotic signal is transduced.[16] In addition, the anti-apoptotic activity of the protein is lost when the RING domain is mutated.[17]

There are interesting subfamilies uniquely possessing two RING fingers. Triad1 (for two RING fingers and DRIL1) and parkin have two RING finger domains separated by the double RING finger linked (DRIL) domain. Triad1 was identified as a nuclear RING finger protein, which is up-regulated during retinoic acid induced granulocytic differentiation of acute leukemia cells.[18] Parkin is a responsible gene for familial autosomal recessive Parkinson's disease.[19,20] Parkin binds to the E2 ubiquitin-conjugating enzymes through its C-terminal RING finger and has ubiquitin–protein ligase activity.[21] Parkin ubiquitinates and promotes the degradation of a putative G protein-coupled transmembrane polypeptide, Pael (parkin-associated endothelial-like) receptor, the insoluble form of which is accumulated in the brains of Parkinson's disease.[22] The insoluble parkin overexpressed in cells causes unfolded protein-induced cell death, whereas coexpression of Parkin suppresses the accumulation of Pael receptor and subsequent cell death.[21] Parkin also ubiquitinates and promotes the degradation of CDCrel-1 (for cell division cycle related-1) and itself.[23] Familial-linked mutations disrupt the ubiquitin–protein ligase function of Parkin and impair Parkin and CDCrel-1 degradation.

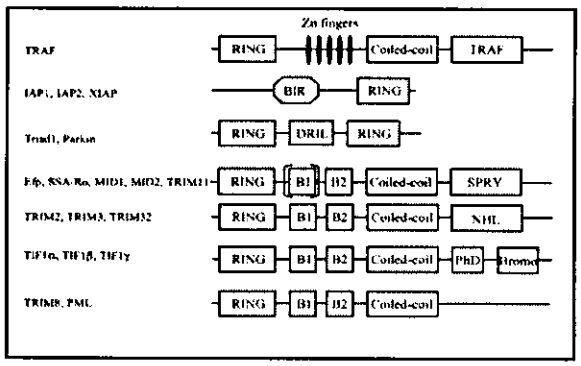

Figure 2. Structures of the RING finger protein family. Representative RING finger proteins with frequently associated domains are presented.

Function of RING Finger

It has been shown in early studies that the RING finger proteins have crucial roles in the growth, differentiation, transcription, signal transduction and oncogenesis.[24] For example, PML is fused to the retinoic acid receptor α (RARα) in acute promyelocytic leukemia (APL) translocation,[25-27] BRCA1 is mutated in early-onset breast cancer and ovarian cancer,[28] TIF1α is a positive cofactor of nuclear hormone receptors[29] and TRAF transduces signals from members of the TNF receptor superfamily to the transcription factor NF-κB.[14] Although those studies appear to show some essential roles played by the RING finger domains in the function of these proteins, the general function of the RING finger domain has not been resolved. However, recently, it was uncovered that the RING finger proteins are involved in the ubiquitin-mediated protein degradation pathway.

The ubiquitin-dependent protein degradation is a specific and sophisticated mechanism in which a target protein to be destroyed is tagged with the ubiquitin. Ubiquitination is accomplished by a complex process involving ubiquitin-activating enzyme (E1), ubiquitin-conjugating enzyme (E2) and ubiquitin ligase (E3).[30] Ubiquitin ligase mediates the transfer of ubiquitin from E2 to a substrate, marking it for degradation by the 26S proteosome. Therefore, E3 enzyme is thought to be important for the specific recognition of the substrate in the ubiquitination pathway. There is accumulating evidence that RING finger domains are identified in E3 complexes and proteins, suggesting the broad use of these domains for ubiquitination. As mentioned above, RING finger domain has the conserved cysteine and histidine residues. The C_3HC_4 type RING finger is found in several E3 proteins including Cbl,[31] BRCA1,[32] Efp (for estrogen-responsive finger protein)[33] and Mdm2 (for murine double minute 2).[34] The RING-H2 subtype is found in Rbx1 (for RING box protein 1) and Apc11 (for anaphase promoting complex (APC) subunit 11) in SCF (Skp1-Cullin-F-box) and APC E3 complexes,[35] respectively, and other ubiquitin ligases. Thus, evidence is accumulating that the RING finger proteins has crucial roles as an E3 ubiquitin ligase in diverse biological functions and diseases. Cbl is one of the initially identified E3 ligase which is involved in the regulation of various tyrosine kinase-linked receptors such as growth factor receptors (for example EGF and PDGF receptors), cytokine receptors and immuno-receptors (for example T-cell, B-cell and Fc-receptors).[36] Cbl recognizes activated protein tyrosine kinases and recruits E2 ubiquitin conjugating enzymes through its SH2 and RING finger domain, respectively. For EGF and PDGF receptors, increased recruitment of Cbl to the activated receptor complex leads to enhanced ubiquitination and degradation of the activated receptor. In contrast, oncogenic mutation in the Cbl RING finger which fails to bind E2 ubiquitin conjugating enzymes abrogates Cbl-mediated EGF receptor ubiquitination and degradation.[37] Thus, it appears that Cbl functions as an adapter to recruit the ubiquitination machinery to activated tyrosine kinase-linked receptors and stimulates receptor ubiquitination and degradation. This causes enhanced down-regulation of the receptor from the cell surface and attenuation of growth factor receptor signaling.

The RING finger protein Mdm2 is identified as an E3 ubiquitin ligase of the tumor-suppressor protein p53 which is a transcription factor and a potent inhibitor of the cell cycle. Mdm2 can bind to p53 and promote its ubiquitination and subsequent degradation by the proteasome.[38,39] It is also known that Mdm2 can ubiquitinate itself, suggesting that some of E3s self-regulate their own stability. The RING finger of Mdm2 is necessary for

both p53 ubiquitin and Mdm2 auto-ubiquitination. Substitution of the Mdm2 RING finger domain with the RING finger from another RING protein maintains the autoubiquination and degradation of Mdm2 but is not able to stimulate p53 ubiquitination. Moreover, mutations in the RING finger domain do not impair binding capacity between Mdm2 and p53. These observations suggest that the RING finger domain appears to be required for specific recognition of substrates in some degree, but is not generally involved in substrate binding.[40]

RBCC/TRIM Subfamily

Frequently, the RING is associated with cysteine-rich B-box domains followed by a predicted coiled coil domain. The B-box domain can be defined as a series of conserved cystein and histidine residues: B1 [Cys-X_2-Cys-X_{7-10}-Cys-X_2-Cys-X_{4-5}-Cys-X_2-Cys/His-X_{3-6}-His-X_{2-8}-His] and B2 [Cys-X_{2-4}-His/Cys-X_{4-9}-Cys-X_2-Cys/His-X_4-Cys/His-X_2-His/Cys] where X can be any amino acid. Structural analysis revealed that it consists of 15 or fewer β-strands.[41] The coiled coil is a common protein motif involving a number of α-helices wound around each other in a highly organized manner and is often used to control oligomerization.[42] These RING, one or two B-boxes and a coiled coil domain motifs are called RBCC or tripartite motif (TRIM)(Fig. 3).[43] This largest subfamily was first identified in a putative transcriptional regulator, Xenopus XNF7[24] and about 50 members have been identified since then. Though either one or two B-boxes are present, the spacing between the RING, B-boxes and the coiled coil is highly conserved with 38-40 residues between the RING and first B-box, and less than 10 amino acids between the second B-box and the coiled coil. There is no apparent homology among these separating sequences. According to the recent progress of genomic analysis, it was revealed that the chromosomal localization of the RBCC/TRIM subfamily genes has an intriguing feature. Although the genes encoding the RBCC/TRIM family members are dispersed throughout the genome, there are two distinct clusters on chromosomes 11p15 and 6p21-22 (Fig. 4). *TRIM22, SSA1/TRIM21, TRIM34, TRIM6, TRIM5, TRIM3* and *SS-56* are clustered in 11p15. *RFP/TRIM27, TRIM31, TRIM10, TRIM15, TRIM26, TRIM38, TRIM39, TRIM40* and *HZFW1* are clustered in 6p21-22. In particular, mRNAs for *TRIM 21, 22* and *34* are shown to be up-regulated by interferons.[44-46] These findings suggest that duplication of an ancestral *RBCC/TRIM* gene at these genomic loci may have occurred and, regulation and function may be conserved to some extents in these genes.[43]

The RBCC/TRIM proteins are associated with certain domains such as B30.2-like or SPRY, NHL, PHD and BROMO domains at their C-terminus. These additional domains may contribute to the function of the subfamily. The B30.2-like domain is a series of 160-170 amino acids containing three highly conserved motifs (LDP, WEVE and LDYE) which is named after the B30-2 exon within the human class I histocompatibility complex locus. The SPRY domain, which was originally named from SPla and the RYanodine Receptor, is composed of around 140 amino acids containing the latter two conserved motifs in B30.2-like domain. At present, the B30.2-like domain is considered as a subclass of the SPRY domain family. The SPRY domain is contained in many of the RBCC/TRIM subfamily including XNF-7, RPT-1, SSA-Ro and STAF50. The significantly conserved SPRY domains imply the biological importance of this gene, however the function of the SPRY domain is not known. The NHL domain name was derived from the three founding members: NCL-1, HT2A, and LIN-41.[47] NCL is involved in rRNA metabolism. HT2A was identified as an interacting partner of the

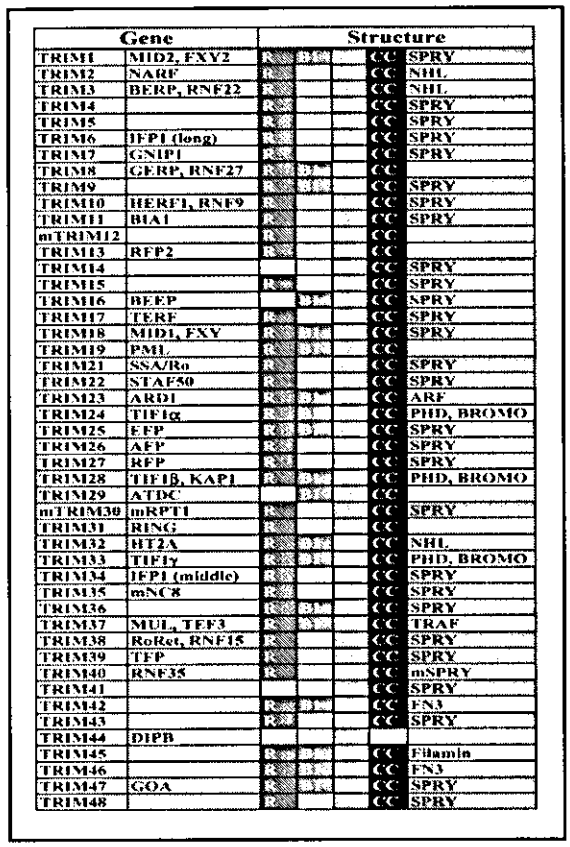

Figure 3. RBCC/TRIM family genes. The gene names are listed in numerical order of *TRIM* genes followed by commonly used names in the second column. Their domain structures are schematically shown to the right.

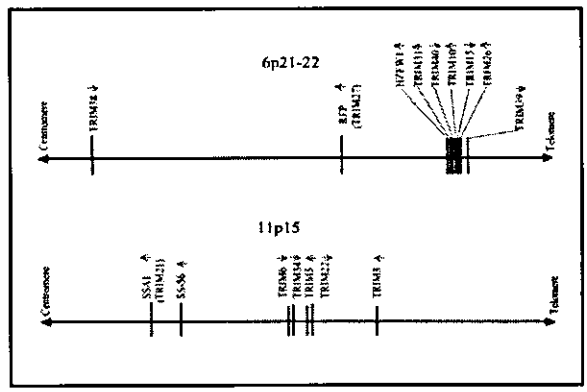

Figure 4. Clustered localization of the *RBCC/TRIM* genes in 6p21-22 and 11p15. *TRIM22, SSA1, TRIM34, TRIM6, TRIM5, TRIM3* and *SS-56* are clustered in 11p15, whereas *RFP, TRIM31, TRIM10, TRIM15, TRIM26, TRIM38, TRIM39, TRIM40* and *HZFW1* are clustered in 6p21-22. The sense strand orientations of each gene are indicated by the arrows.

HIV Tat protein and Lin41 is involved in posttranscriptional regulation of mRNA. The NHL motif has a slight homology with WD40 domain, suggesting a protein-protein interaction. The C-terminal PHD fingers and bromodomains are found in TIF1α and KAP1/TIF1β. The PHD domain is a motif characteristically defined by seven cysteines and a histidine that are highly homologous to the RING motif and is contained in some transcription factors. The PHD domain of MEKK1 (MEK kinase 1) exhibited E3 ubiquitin ligase activity toward ERK (extracellular signal-regulated protein kinase) 2, suggesting a negative regulatory mechanism for decreasing ERK1/2 activity.[48] The bromodomain is also found in transcription factors, can bind histones with acetylated lysines and appears to be involved in chromatin remodeling.[49] KAP1/TIF1β and TIF1α are involved in transcriptional regulation. Genes belonging to this RBCC/TRIM family are implicated in a variety of processes such as development and cell growth and are involved in several human diseases. PYRIN,[50] MID1 (Midline 1)[51] and MUL (for mulibrey nanism proteins)[52] are mutated in familial Mediterranean fever, X-linked Opitz/GBBB syndrome and mulibrey nanism, respectively, whereas PML, RFP (ret finger protein) and TIF1α acquire oncogenic activity when fused to RARα, RET or B-raf, respectively.

It has been shown that the RBCC/TRIM proteins can oligomerize through their coiled coil domains. In homodimerization of RFP proteins, the coiled coil region with the B-box but not the RING finger is required.[53] In this case, while the B-box is not an interacting interface itself, the mutation of conserved cysteine residues within the B-box affects the ability of RFP to multimerize, suggesting that its structural integrity is necessary for this interaction to occur.[53] The coiled coil domain of RFP is also necessary for interaction with Enhancer of polycomb protein (EPC) to repress gene transcription.[54] The homodimerization and binding with EPC occurs with the proximal coil in RFP protein. RFP also directly interacts and colocalizes with PML in a subset of the PML NBs (nuclear bodies).[55] This interaction is mediated by the RFP B-box and the distal two coils. The association of RFP with the PML NBs is altered by mutations that affect RFP/PML interaction and in APL patients-derived cells. These results indicate that RFP have an important role in regulating cellular growth and differentiation. MID1 protein, which is mutated in patients with Opitz GBBB syndrome, and the highly related gene MID2 also make both homo- and hetero-dimers mediated by the coiled coil motifs. The dimerization is a prerequisite for the association of MID and Alpha 4 (a regulatory subunit of PP2-type phosphatases) and the complex formation with microtubules which seems important for normal midline development.[56] In contrast, it has been shown that the entire RBCC/TRIM domain is required for hetero-oligomerization or binding natural ligands. The RBCC region of KAP1/TIF1β associates with the KRAB (Krüppel-associated box) transcriptional repressor domain of KOX-1.[57] From extensive studies of the interaction, it has been revealed that the interaction is specific for the KAP1 RBCC/TRIM domain. Namely, when each RBCC/TRIM motifs of KAP1 was swapped with other corresponding ones of MID1, KAP1 did not bind the KRAB domain any more. Therefore, each domain of the RBCC may function as an independent functional unit and have important roles in the specific recognition of interacting partners or oligomers formation. In other RBCC/TRIM proteins, only one copy of the B-box motif is present, but inspection of the whole family reveals a conserved residue spacing between the RING, B-box and coiled coil domains.[43] This strongly suggests that the overall architecture of the RBCC/TRIM motif is highly conserved, perhaps relating to the motif acting as a scaffold for higher-order protein-protein interactions.[57] Molecular modeling suggests that the position and orientation of the B-box (adjacent to the coiled coil) would be critical for the correct alignment of the α-helices that form the coiled coil. Interestingly, unlike the RING and coiled coil motifs, the B-box is only found in RBCC/TRIM family members suggesting that it is a critical determinant of the overall motif and its function.[43]

As mentioned above, the latest findings of RING fingers in E3 ubiquitin ligases imply that the members of this RBCC/TRIM subfamily are potential candidates for specific regulators/adopters in ubiquitin-dependent protein degradation. In fact, some genes belonging to the subfamily has been proven to act as E3 ligase. We next discuss such genes focusing on the recent findings.

Ring Fingers that Act As E3 Ligases

Efp

Estrogen-responsive finger protein (Efp) is a member of the RING-finger, B1 and B2-boxes, coiled coil and SPRY (RBCC-SPRY) subfamily in the RING finger family. Efp was isolated as an estrogen-responsive gene by genomic binding-site cloning using a recombinant estrogen receptor (ER) protein.[58] The estrogen-responsive element (ERE) to which ER can bind is found at the 3'-untranslated region (UTR) in the *Efp* gene and the gene's expression is predominantly detected in female reproductive organs including uterus, ovary and mammary gland[59] and in breast and ovarian cancers.[60] Estrogen-induced expression is found in the uterus, brain and mammary gland cells. *Efp* knockout mice have an underdeveloped uterus and estrogen responses of uterin cells from knockout mice are markedly attenuated, suggesting that Efp is necessary for estrogen-induced cell growth.[61] Moreover, tumor growth of breast cancer MCF7 cells implanted in female athymic mice has been demonstrated to be reduced by treatment with antisense Efp oligonucleotide. In contrast, Efp-overexpressing MCF7 cells in ovariectomized athymic mice generate tumors in the absence of estrogen.[33] These results indicate that Efp mediaes estrogen-dependent growth in breast cancer cells. We identified 14-3-3Σ which is responsible for reduced cell growth, as a binding factor to Efp and found an accumulation of 14-3-3Σ in *Efp* knockout mouse embryonic fibroblasts. Furthermore, it has been revealed that Efp is an ubiquitin ligase (E3) that targets proteolysis of 14-3-3Σ. Specifically, the RING which preferentially bound to ubiquitin-conjugating enzyme UbcH8 has been shown to be essential for the ubiquitination of 14-3-3Σ. Our findings provide an insight into the cell-cycle machinery and tumorigenesis of breast cancer by identifying 14-3-3Σ as a target for proteolysis by Efp, leading to cell proliferation. The degradation of 14-3-3Σ is subsequently followed by dissociation of the protein from cyclin–Cdk complexes, leading to cell cycle progression and tumor growth (Fig. 5).

MID1, MID2

Opitz GBBB syndrome (OS; Opitz syndrome) is a genetically and phenotypically complex disorder defined by characteristic facial anomalies, structural heart defects, as well as anal and genital anomalies.[62,63] A positional cloning approach has revealed a candidate gene designated *MID1*[51] which is a member of the RBCC-SPRY family. Most of the mutations identified so far in patients with Opitz syndrome cluster in the SPRY domain of

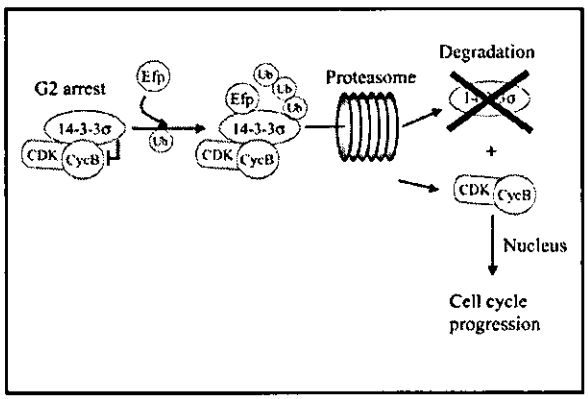

Figure 5. Models of Efp action as E3 ligase. Estrogen-induced RING finger protein Efp recognizes a cell cycle inhibitor 14-3-3Σ which keeps Cyclin B in cytoplasm. Efp modifies 14-3-3Σ with ubiquitin and the resulting ubiquitinated 14-3-3Σ is recruited to 26S proteosome to be destroyed. The dissociated cyclin B is now capable of entering the nucleus where it drives cell cycle.

MID1. It has been shown that MID1 associates with microtubules, whereas mutant forms of MID1 do not.[64] These results suggest that MID1 has a physiological role in microtubule dynamics.

Recently, the α4 protein, a regulatory subunit of protein phosphatase 2A (PP2A)[65] was isolated by yeast two-hybrid screening with MID1 as bait. It was demonstrated that the B-box 1 is sufficient for a strong interaction with α4. MID2,[66] which is highly similar to MID1, also binds α4. Cellular localizations of MID1 and α4 are coincident with cytoskeletal structures and MID1 with a mutation at the C terminus that mimics the mutant protein of some individuals with OS results in the formation of cytoplasmic clumps containing both proteins. The identified substrate for E3 ligase activity of MID1 is a cytosolic PP2A. In contrast, addition of a proteasomé inhibitor to OS-derived fibroblasts expressing dysfunctional MID1 does not cause either enrichment of PP2A or accumulation of the enzyme's polyubiquitinated forms,[67] suggesting that MID1 mutations result in decreased proteolysis of the C subunit of PP2A in individuals with OS.

PML

PML also belongs to a subfamily of proteins containing a RBCC/TRIM motif.[43,68] PML has been implicated in the pathogenesis of acute promyelocytic leukemia that arises following a reciprocal chromosomal translocation that fuses the *PML* gene located on chromosome 15 with the retinoic acid receptor alpha (*RARα*) gene located on chromosome 17. The resulting PML-RARα fusion protein preserves most of the functional domains of both PML and RARα, but it lacks C-terminus of PML and N-terminus of RARα The fusion protein shows cell type- and promoter-specific differences from the wild type RARα,[25,26,69] while it maintains a responsiveness to retinoic acid. Overexpression of PML-RARα inhibits vitamin D3 and transforming growth factor β-induced differentiation and also reduces serum starvation-induced apoptosis in U937 cells.[70] In addition, dimerization of PML with PML-RARα is required to block differentiation.[71] Thus, PML-RARα is considered to function as a dominant negative protein by interfering with the function of PML and RARα.

In normal cells, cellular distribution of PML is found to form a discrete subnuclear compartment (nuclear body, NB)[72,73] or PML oncogenic domain.[74] Other proteins containing Sp100[75] and PLZF (for promyelocytic leukemia zinc finger)[76] have been reported to localize to the NBs. Interestingly, PLZF-RARα fusion protein is also found in a rare form of APL.[77] It is shown that the nuclear bodies were dispersed into a microspeckle pattern in APL cells but reformed with retinoic acid treatment by which APL cells differentiated into granulocytes. In addition, the NB is the preferred site where the early steps of transcription and replication of DNA virus occurs.[78] Therefore, the regulation of NB formation is thought to be involved in the pathogenesis of APL. Recently, PML is shown to be covalently modified by SUMO-1 (Small Ubiquitin-like Modifier-1) of ubiquitin-like proteins.[79] Mutations in the PML RING finger disrupt the nuclear body formation in vivo[3,69] and cause a failure of growth suppression,[80,81] apoptosis and anti-viral activities[82] of PML. The dependence on an intact RING finger for PML NBs formation implies specific protein interactions regulated by the RING structure. Recent studies have shown that PML RING interacting with the SUMO-1 E2 enzyme UBC9 is SUMO modified and the sumolylation of PML has an important role in regulating the formation of NBs.[83]

PML has two B-boxes (B1 and B2) adjacent to the RING domain. Mutations of conserved zinc-chelating residues in B1 and/or B2 boxes collapsed PML NB formation, whereas they did not affect PML oligomerization.[84] PML B-boxes are also involved in growth suppression.[80] It has been revealed that PML is sumoylated in B1 box which is responsible for binding of the 11S proteasomal subunit to PML NBs.[85]

The coiled coil region in PML is indispensable for multimerization or heterodimerization with PML-RARα,[69,71,86] formation of PML NB and growth suppression activity.[80] Notably, the important role of the coiled coil domain for the complex formation is also suggested from the studies of other RBCC/TRIM subfamily.[43,57]

TRIM8

TRIM8, a member of RBCC subfamily, is shown to interact with SOCS-1 (suppressor of cytokine signaling-1) which is induced by cytokines and inhibits cytokine signaling by binding to downstream signaling molecules such as JAK (Janus kinase) kinases.[87-89] The B-box coiled coil region of TRIM8 is sufficient for efficient interaction with SOCS-1, but the RING portion of the protein is not required for the binding. By contrast, both the SOCS box and the SH2 domain in SOCS-1 appear to be necessary for the interaction between SOCS-1 and TRIM8. It was found that exogenous coexpression of TRIM8/GERP with SOCS-1 decreased the stability of SOCS-1 protein and TRIM8 restored the IFN-γ-mediated transcription which was inhibited by the expression of SOCS-1.[90] These results suggest that TRIM8 is the putative E3 ligase for SOCS-1 and inhibits SOCS-1 function by targeting it for proteasomal degradation.

TRIM11

TRIM11 is a member of the protein family composed of a RING finger domain, which is a putative E3 ubiquitin ligase, a B-box domain, a coiled coil domain and a SPRY domain. A recent experiment with yeast two-hybrid screening has revealed that TRIM11 can interact with Humanin[91] which is a newly identified anti-apoptotic peptide that specifically suppresses Alzheimer's disease (AD)-related neurotoxicity. It is known that Bax

(Bcl2-associated X protein) has a crucial role in apoptosis. In response to death stimuli, Bax protein changes the conformation exposing membrane-targeting domains, translocates to mitochondrial membrane and releases the cytochrome c and other apoptogenic proteins. Indeed, Humanin is shown to bind with Bax and prevents the translocation of Bax from cytosol to mitochondria.[92] Moreover, Humanin blocks Bax association with isolated mitochondria and suppresses cytochrome c release. Therefore, Humanin seems to exert its anti-apoptotic effect by interfering the Bax function.

The coiled coil domain of TRIM11 is indispensable for the interaction with Humanin. The SPRY domain also contributes to the recognition of Humanin, whereas SPRY domain alone cannot. It was found that the intracellular level of Humanin was drastically reduced by the coexpression of TRIM11, and mutation of the RING finger domain or treatment with proteasome inhibitor attenuates the effect of TRIM11 on the intracellular level of Humanin.[91] These results suggest that the TRIM11 participates in the ubiquitin-mediated degradation of Humanin as an E3 ligase.

SSA/Ro (SSA1, TRIM21)

Sjögren syndrome is an autoimmune disease in which exocrine glands including salivary and lacrimal glands develop a chronic inflammation, and whose symptoms are dry eyes, dry mouth and fatigue. Autoantibodies to Ro recognize a ribonucleoprotein complex composed of small single-stranded RNAs and of one or more peptides. Although the Ro autoantigen is heterogeneous and found in most tissues and cells with differences in structure and quantity across tissues, it is detected in 35 to 50% of patients with systemic lupus erythematosus and in up to 97% of patients with Sjögren syndrome.[93] The 60-kD protein (Ro60) and the 52-kD protein (Ro52) were identified[94] and, another novel 56-kD protein (Ro56/SS-56) has been identified, recently.[95] Ro52 and Ro56 proteins belong to RBCC-SPRY subfamily. It is thought that the Ro autoantigen is involved in the regulation of transcription because it possesses functional domains associated with gene-regulation and binds to nucleic acids.[93] Its precise function is not understood, however. In a study, Ro52 was reported to be ubiquitinated in the cell.[96] The observation suggests that Ro52 may be downregulated by the ubiquitin–proteasome pathway in vivo. Interestingly, sera from patients with Sjögren syndrome showed heterogeneity in their reactivity to poly-ubiquitinated Ro52, probably because of their differing antigenic determinants. This heterogeneity of the reactivity may be associated with the varying clinical features found in Sjögren patients.

Conclusion

Here, we summarized the structural characteristics and functions of RING finger proteins specifically in terms of the E3 ligase activity. However, relatively few proteins have been really proven to function as E3 ligase. Thus, most RING finger proteins remain to be further investigated. Investigation of the RING finger proteins as a novel E3 ligase family will elucidate important mechanisms of cellular protein degradation and provide new insight into the physiological and pathophysiological roles of the pathway. Particularly, the molecular mechanisms of specific substrate recognition by E3 with the RING and other associated domains must be determined. Moreover, the RING finger proteins such as PML may possess unknown functions other than E3 ligase. Functional analysis of the RING finger proteins will help to understand biological roles of the family including the ubiquitin-mediated protein degradation pathway.

References

1. Freemont PS, Hanson IM, Trowsdale J. A novel cysteine-rich sequence motif. Cell 1991; 64(3):483-484.
2. Lovering R, Hanson IM, Borden KL et al. Identification and preliminary characterization of a protein motif related to the zinc finger. Proc Natl Acad Sci USA 1993; 90(6):2112-2116.
3. Borden KL, Boddy MN, Lally J et al. The solution structure of the RING finger domain from the acute promyelocytic leukaemia proto-oncoprotein PML. Embo J 1995; 14(7):1532-1541.
4. Barlow PN, Luisi B, Milner A et al. Structure of the C3HC4 domain by 1H-nuclear magnetic resonance spectroscopy. A new structural class of zinc-finger. J Mol Biol 1994; 237(2):201-211.
5. Bellon SF, Rodgers KK, Schatz DG et al. Crystal structure of the RAG1 dimerization domain reveals multiple zinc-binding motifs including a novel zinc binuclear cluster. Nat Struct Biol 1997; 4(7):586-591.
6. Gervais V, Busso D, Wasielewski E et al. Solution structure of the N-terminal domain of the human TFIIH MAT1 subunit: New insights into the RING finger family. J Biol Chem 2001; 276(10):7457-7464.
7. Zheng N, Wang P, Jeffrey PD et al. Structure of a c-Cbl-UbcH7 complex: RING domain function in ubiquitin-protein ligases. Cell 2000; 102(4):533-539.
8. Freemont PS. The RING finger. A novel protein sequence motif related to the zinc finger. Ann N Y Acad Sci 1993; 684:174-192.
9. Saurin AJ, Borden KL, Boddy MN et al. Does this have a familiar RING? Trends Biochem Sci 1996; 21(6):208-214.
10. Takeuchi M, Rothe M, Goeddel DV. Anatomy of TRAF2. Distinct domains for nuclear factor-kappaB activation and association with tumor necrosis factor signaling proteins. J Biol Chem 1996; 271(33):19935-19942.
11. Sato T, Irie S, Reed JC. A novel member of the TRAF family of putative signal transducing proteins binds to the cytosolic domain of CD40. FEBS Lett 1995; 358(2):113-118.
12. Cheng G, Cleary AM, Ye ZS et al. Involvement of CRAF1, a relative of TRAF, in CD40 signaling. Science 1995; 267(5203):1494-1498.
13. Rothe M, Sarma V, Dixit VM et al. TRAF2-mediated activation of NF-kappa B by TNF receptor 2 and CD40. Science 1995; 269(5229):1424-1427.
14. Takahashi R, Deveraux Q, Tamm I et al. A single BIR domain of XIAP sufficient for inhibiting caspases. J Biol Chem 1998; 273(14):7787-7790.
15. Liston P, Fong WG, Kelly NL et al. Identification of XAF1 as an antagonist of XIAP anti-Caspase activity. Nat Cell Biol 2001; 3(2):128-133.
16. Yang Y, Fang S, Jensen JP et al. Ubiquitin protein ligase activity of IAPs and their degradation in proteasomes in response to apoptotic stimuli. Science 2000; 288(5467):874-877.
17. Clem RJ, Miller LK. Control of programmed cell death by the baculovirus genes p35 and iap. Mol Cell Biol 1994; 14(8):5212-5222.
18. van der Reijden BA, Erpelinck-Verschueren CA, Lowenberg B et al. TRIADs: A new class of proteins with a novel cysteine-rich signature. Protein Sci 1999; 8(7):1557-1561.
19. Kitada T, Asakawa S, Hattori N et al. Mutations in the parkin gene cause autosomal recessive juvenile parkinsonism. Nature 1998; 392(6676):605-608.
20. Morett E, Bork P. A novel transactivation domain in parkin. Trends Biochem Sci 1999; 24(6):229-231.
21. Imai Y, Soda M, Inoue H et al. An unfolded putative transmembrane polypeptide, which can lead to endoplasmic reticulum stress, is a substrate of Parkin. Cell 2001; 105(7):891-902.
22. Imai Y, Soda M, Hatakeyama S et al. CHIP is associated with Parkin, a gene responsible for familial Parkinson's disease, and enhances its ubiquitin ligase activity. Mol Cell 2002; 10(1):55-67.

23. Zhang Y, Gao J, Chung KK et al. Parkin functions as an E2-dependent ubiquitin- protein ligase and promotes the degradation of the synaptic vesicle-associated protein, CDCrel-1. Proc Natl Acad Sci USA 2000; 97(24):13354-13359.
24. Reddy BA, Etkin LD, Freemont PS. A novel zinc finger coiled-coil domain in a family of nuclear proteins. Trends Biochem Sci 1992; 17(9):344-345.
25. Kakizuka A, Miller Jr WH, Umesono K et al. Chromosomal translocation t(15;17) in human acute promyelocytic leukemia fuses RAR alpha with a novel putative transcription factor, PML. Cell 1991; 66(4):663-674.
26. de The H, Lavau C, Marchio A et al. The PML-RAR alpha fusion mRNA generated by the t(15;17) translocation in acute promyelocytic leukemia encodes a functionally altered RAR. Cell 1991; 66(4):675-684.
27. Goddard AD, Borrow J, Freemont PS et al. Characterization of a zinc finger gene disrupted by the t(15;17) in acute promyelocytic leukemia. Science 1991; 254(5036):1371-1374.
28. Miki Y, Swensen J, Shattuck-Eidens D et al. A strong candidate for the breast and ovarian cancer susceptibility gene BRCA1. Science 1994; 266(5182):66-71.
29. Le Douarin B, Zechel C, Garnier JM et al. The N-terminal part of TIF1, a putative mediator of the ligand-dependent activation function (AF-2) of nuclear receptors, is fused to B-raf in the oncogenic protein T18. Embo J 1995; 14(9):2020-2033.
30. Hershko A, Ciechanover A. The ubiquitin system. Annu Rev Biochem 1998; 67:425-479.
31. Joazeiro CA, Wing SS, Huang H et al. The tyrosine kinase negative regulator c-Cbl as a RING-type, E2-dependent ubiquitin-protein ligase. Science 1999; 286(5438):309-312.
32. Lorick KL, Jensen JP, Fang S et al. RING fingers mediate ubiquitin-conjugating enzyme (E2)-dependent ubiquitination. Proc Natl Acad Sci USA 1999; 96(20):11364-11369.
33. Urano T, Saito T, Tsukui T et al. Efp targets 14-3-3 sigma for proteolysis and promotes breast tumour growth. Nature 2002; 417(6891):871-875.
34. Zhang Y, Xiong Y. Control of p53 ubiquitination and nuclear export by MDM2 and ARF. Cell Growth Differ 2001; 12(4):175-186.
35. Seol JH, Feldman RM, Zachariae W et al. Cdc53/cullin and the essential Hrt1 RING-H2 subunit of SCF define a ubiquitin ligase module that activates the E2 enzyme Cdc34. Genes Dev 1999; 13(12):1614-1626.
36. Galisteo ML, Dikic I, Batzer AG et al. Tyrosine phosphorylation of the c-cbl proto-oncogene protein product and association with epidermal growth factor (EGF) receptor upon EGF stimulation. J Biol Chem 1995; 270(35):20242-20245.
37. Thien CB, Walker F, Langdon WY. RING finger mutations that abolish c-Cbl-directed polyubiquitination and downregulation of the EGF receptor are insufficient for cell transformation. Mol Cell 2001; 7(2):355-365.
38. Haupt Y, Maya R, Kazaz A et al. Mdm2 promotes the rapid degradation of p53. Nature 1997; 387(6630):296-299.
39. Kubbutat MH, Jones SN, Vousden KH. Regulation of p53 stability by Mdm2. Nature 1997; 387(6630):299-303.
40. Geyer RK, Yu ZK, Maki CG. The MDM2 RING-finger domain is required to promote p53 nuclear export. Nat Cell Biol 2000; 2(9):569-573.
41. Chen Y, Chen CF, Riley DJ et al. Aberrant subcellular localization of BRCA1 in breast cancer. Science 1995; 270(5237):789-791.
42. Lupas A. Coiled coils: New structures and new functions. Trends Biochem Sci 1996; 21(10):375-382.
43. Reymond A, Meroni G, Fantozzi A et al. The tripartite motif family identifies cell compartments. Embo J 2001; 20(9):2140-2151.
44. Tissot C, Mechti N. Molecular cloning of a new interferon-induced factor that represses human immunodeficiency virus type 1 long terminal repeat expression. J Biol Chem 1995; 270(25):14891-14898.
45. Der SD, Zhou A, Williams BR et al. Identification of genes differentially regulated by interferon alpha, beta, or gamma using oligonucleotide arrays. Proc Natl Acad Sci USA 1998; 95(26):15623-15628.
46. Orimo A, Tominaga N, Yoshimura K et al. Molecular cloning of ring finger protein 21 (RNF21)/interferon-responsive finger protein (ifp1), which possesses two RING-B box-coiled coil domains in tandem. Genomics 2000; 69(1):143-149.
47. Slack FJ, Ruvkun G. A novel repeat domain that is often associated with RING finger and B-box motifs. Trends Biochem Sci 1998; 23(12):474-475.
48. Lu Z, Xu S, Joazeiro C et al. The PHD domain of MEKK1 acts as an E3 ubiquitin ligase and mediates ubiquitination and degradation of ERK1/2. Mol Cell 2002; 9(5):945-956.
49. Dhalluin C, Carlson JE, Zeng L et al. Structure and ligand of a histone acetyltransferase bromodomain. Nature 1999; 399(6735):491-496.
50. Ancient missense mutations in a new member of the RoRet gene family are likely to cause familial Mediterranean fever. The International FMF Consortium. Cell 1997; 90(4):797-807.
51. Quaderi NA, Schweiger S, Gaudenz K et al. Opitz G/BBB syndrome, a defect of midline development, is due to mutations in a new RING finger gene on Xp22. Nat Genet 1997; 17(3):285-291.
52. Avela K, Lipsanen-Nyman M, Idanheimo N et al. Gene encoding a new RING-B-box-Coiled-coil protein is mutated in mulibrey nanism. Nat Genet 2000; 25(3):298-301.
53. Cao T, Borden KL, Freemont PS et al. Involvement of the rfp tripartite motif in protein-protein interactions and subcellular distribution. J Cell Sci 1997; 110(Pt 14):1563-1571.
54. Shimono Y, Murakami H, Hasegawa Y et al. RET finger protein is a transcriptional repressor and interacts with enhancer of polycomb that has dual transcriptional functions. J Biol Chem 2000; 275(50):39411-39419.
55. Cao T, Duprez E, Borden KL et al. Ret finger protein is a normal component of PML nuclear bodies and interacts directly with PML. J Cell Sci 1998; 111(Pt 10):1319-1329.
56. Trockenbacher A, Suckow V, Foerster J et al. MID1, mutated in Opitz syndrome, encodes an ubiquitin ligase that targets phosphatase 2A for degradation. Nat Genet 2001; 29(3):287-294.
57. Peng H, Begg GE, Schultz DC et al. Reconstitution of the KRAB-KAP-1 repressor complex: A model system for defining the molecular anatomy of RING-B box-coiled-coil domain-mediated protein-protein interactions. J Mol Biol 2000; 295(5):1139-1162.
58. Inoue S, Orimo A, Hosoi T et al. Genomic binding-site cloning reveals an estrogen-responsive gene that encodes a RING finger protein. Proc Natl Acad Sci USA 1993; 90(23):11117-11121.
59. Orimo A, Inoue S, Ikeda K et al. Molecular cloning, structure, and expression of mouse estrogen-responsive finger protein Efp. Colocalization with estrogen receptor mRNA in target organs. J Biol Chem 1995; 270(41):24406-24413.
60. Ikeda K, Orimo A, Higashi Y et al. Efp as a primary estrogen-responsive gene in human breast cancer. FEBS Lett 2000; 472(1):9-13.
61. Orimo A, Inoue S, Minowa O et al. Underdeveloped uterus and reduced estrogen responsiveness in mice with disruption of the estrogen-responsive finger protein gene, which is a direct target of estrogen receptor alpha. Proc Natl Acad Sci USA 1999; 96(21):12027-12032.
62. Opitz JM. G syndrome (hypertelorism with esophageal abnormality and hypospadias, or hypospadias-dysphagia, or "Opitz-Frias" or "Opitz-G" syndrome)—perspective in 1987 and bibliography. Am J Med Genet 1987; 28(2):275-285.
63. Robin NH, Opitz JM, Muenke M. Opitz G/BBB syndrome: Clinical comparisons of families linked to Xp22 and 22q, and a review of the literature. Am J Med Genet 1996; 62(3):305-317.
64. Gaudenz K, Roessler E, Quaderi N et al. Opitz G/BBB syndrome in Xp22: Mutations in the MID1 gene cluster in the carboxy-terminal domain. Am J Hum Genet 1998; 63(3):703-710.
65. Jerome LA, Papaioannou VE. DiGeorge syndrome phenotype in mice mutant for the T-box gene, Tbx1. Nat Genet 2001; 27(3):286-291.
66. Cainarca S, Messali S, Ballabio A et al. Functional characterization of the Opitz syndrome gene product (midin): Evidence for homodimerization and association with microtubules throughout the cell cycle. Hum Mol Genet 1999; 8(8):1387-1396.

67. Short KM, Hopwood B, Yi Z et al. MID1 and MID2 homo- and heterodimerise to tether the rapamycin-sensitive PP2A regulatory subunit, alpha 4, to microtubules: Implications for the clinical variability of X-linked Opitz GBBB syndrome and other developmental disorders. BMC Cell Biol 2002; 3(1):1.
68. Borden KL. RING fingers and B-boxes: Zinc-binding protein-protein interaction domains. Biochem Cell Biol 1998; 76(2-3):351-358.
69. Kastner P, Perez A, Lutz Y et al. Structure, localization and transcriptional properties of two classes of retinoic acid receptor alpha fusion proteins in acute promyelocytic leukemia (APL): Structural similarities with a new family of oncoproteins. Embo J 1992; 11(2):629-642.
70. Grignani F, Ferrucci PF, Testa U et al. The acute promyelocytic leukemia-specific PML-RAR alpha fusion protein inhibits differentiation and promotes survival of myeloid precursor cells. Cell 1993; 74(3):423-431.
71. Grignani F, Testa U, Rogaia D et al. Effects on differentiation by the promyelocytic leukemia PML/RARalpha protein depend on the fusion of the PML protein dimerization and RARalpha DNA binding domains. Embo J 1996; 15(18):4949-4958.
72. Weis K, Rambaud S, Lavau C et al. Retinoic acid regulates aberrant nuclear localization of PML-RAR alpha in acute promyelocytic leukemia cells. Cell 1994; 76(2):345-356.
73. Koken MH, Puvion-Dutilleul F, Guillemin MC et al. The t(15;17) translocation alters a nuclear body in a retinoic acid-reversible fashion. Embo J 1994; 13(5):1073-1083.
74. Dyck JA, Maul GG, Miller Jr WH et al. A novel macromolecular structure is a target of the promyelocyte-retinoic acid receptor oncoprotein. Cell 1994; 76(2):333-343.
75. Szostecki C, Guldner HH, Netter HJ et al. Isolation and characterization of cDNA encoding a human nuclear antigen predominantly recognized by autoantibodies from patients with primary biliary cirrhosis. J Immunol 1990; 145(12):4338-4347.
76. Koken MH, Reid A, Quignon F et al. Leukemia-associated retinoic acid receptor alpha fusion partners, PML and PLZF, heterodimerize and colocalize to nuclear bodies. Proc Natl Acad Sci USA 1997; 94(19):10255-10260.
77. Chen Z, Brand NJ, Chen A et al. Fusion between a novel Kruppel-like zinc finger gene and the retinoic acid receptor-alpha locus due to a variant t(11;17) translocation associated with acute promyelocytic leukaemia. Embo J 1993; 12(3):1161-1167.
78. Ishov AM, Maul GG. The periphery of nuclear domain 10 (ND10) as site of DNA virus deposition. J Cell Biol 1996; 134(4):815-826.
79. Kamitani T, Nguyen HP, Kito K et al. Covalent modification of PML by the sentrin family of ubiquitin-like proteins. J Biol Chem 1998; 273(6):3117-3120.
80. Fagioli M, Alcalay M, Tomassoni L et al. Cooperation between the RING + B1-B2 and coiled-coil domains of PML is necessary for its effects on cell survival. Oncogene 1998; 16(22):2905-2913.
81. Mu ZM, Chin KV, Liu JH et al. PML, a growth suppressor disrupted in acute promyelocytic leukemia. Mol Cell Biol 1994; 14(10):6858-6867.
82. Regad T, Saib A, Lallemand-Breitenbach V et al. PML mediates the interferon-induced antiviral state against a complex retrovirus via its association with the viral transactivator. Embo J 2001; 20(13):3495-3505.
83. Kamitani T, Kito K, Nguyen HP et al. Identification of three major sentrinization sites in PML. J Biol Chem 1998; 273(41):26675-26682.
84. Borden KL, Lally JM, Martin SR et al. In vivo and in vitro characterization of the B1 and B2 zinc-binding domains from the acute promyelocytic leukemia protooncoprotein PML. Proc Natl Acad Sci USA 1996; 93(4):1601-1606.
85. Lallemand-Breitenbach V, Zhu J, Puvion F et al. Role of promyelocytic leukemia (PML) sumolation in nuclear body formation, 11S proteasome recruitment, and As2O3-induced PML or PML/retinoic acid receptor alpha degradation. J Exp Med 2001; 193(12):1361-1371.
86. Le XF, Yang P, Chang KS. Analysis of the growth and transformation suppressor domains of promyelocytic leukemia gene, PML. J Biol Chem 1996; 271(1):130-135.
87. Chen XP, Losman JA, Rothman P. SOCS proteins, regulators of intracellular signaling. Immunity 2000; 13(3):287-290.
88. Haque SJ, Harbor PC, Williams BR. Identification of critical residues required for suppressor of cytokine signaling-specific regulation of interleukin-4 signaling. J Biol Chem 2000; 275(34):26500-26506.
89. Terstegen L, Maassen BG, Radtke S et al. Differential inhibition of IL-6-type cytokine-induced STAT activation by PMA. FEBS Lett 2000; 478(1-2):100-104.
90. Toniato E, Chen XP, Losman J et al. TRIM8/GERP RING finger protein interacts with SOCS-1. J Biol Chem 2002; 277(40):37315-37322.
91. Niikura T, Hashimoto Y, Tajima H et al. A tripartite motif protein TRIM11 binds and destabilizes Humanin, a neuroprotective peptide against Alzheimer's disease-relevant insults. Eur J Neurosci 2003; 17(6):1150-1158.
92. Guo B, Zhai D, Cabezas E et al. Humanin peptide suppresses apoptosis by interfering with Bax activation. Nature 2003; 423(6938):456-461.
93. Sibilia J. Ro(SS-A) and anti-Ro(SS-A): An update. Rev Rhum Engl Ed 1998; 65(1):45-57.
94. Itoh Y, Reichlin M. Autoantibodies to the Ro/SSA antigen are conformation dependent. I: Anti-60 kD antibodies are mainly directed to the native protein; anti-52 kD antibodies are mainly directed to the denatured protein. Autoimmunity 1992; 14(1):57-65.
95. Billaut-Mulot O, Cocude C, Kolesnitchenko V et al. SS-56, a novel cellular target of autoantibody responses in Sjogren syndrome and systemic lupus erythematosus. J Clin Invest 2001; 108(6):861-869.
96. Fukuda-Kamitani T, Kamitani T. Ubiquitination of Ro52 autoantigen. Biochem Biophys Res Commun 2002; 295(4):774-778.

THE JOURNAL OF BIOLOGICAL CHEMISTRY
Vol. 278, No. 50, Issue of December 12, pp. 50226–50233, 2003
Printed in U.S.A.

Glutaredoxin Exerts an Antiapoptotic Effect by Regulating the Redox State of Akt*

Received for publication, September 12, 2003
Published, JBC Papers in Press, October 1, 2003, DOI 10.1074/jbc.M310171200

Hiroaki Murata‡§, Yoshito Ihara‡¶, Hajime Nakamura‖, Junji Yodoi‖, Koji Sumikawa§, and Takahito Kondo‡

From the ‡Department of Biochemistry and Molecular Biology in Disease, Atomic Bomb Disease Institute and the §Department of Anesthesiology, Nagasaki University School of Medicine, 1-12-4 Sakamoto, Nagasaki, 852-8523 and the ‖Department of Biological Responses, Institute for Viral Research, Kyoto University, 53 Shogoin, Kawahara-cho, Sakyo-ku, Kyoto, 606-8507, Japan

Glutaredoxin (GRX) is a small dithiol protein involved in various cellular functions, including the redox regulation of certain enzyme activities. GRX functions via a disulfide exchange reaction by utilizing the active site Cys-Pro-Tyr-Cys. Here we demonstrated that overexpression of GRX protected cells from hydrogen peroxide (H_2O_2)-induced apoptosis by regulating the redox state of Akt. Akt was transiently phosphorylated, dephosphorylated, and then degraded in cardiac H9c2 cells undergoing H_2O_2-induced apoptosis. Under stress, Akt underwent disulfide bond formation between Cys-297 and Cys-311 and dephosphorylation in accordance with an increased association with protein phosphatase 2A. Overexpression of GRX protected Akt from H_2O_2-induced oxidation and suppressed recruitment of protein phosphatase 2A to Akt, resulting in a sustained phosphorylation of Akt and inhibition of apoptosis. This effect was reversed by cadmium, an inhibitor of GRX. Furthermore an *in vitro* assay revealed that GRX reduced oxidized Akt in concert with glutathione, NADPH, and glutathione-disulfide reductase. Thus, GRX plays an important role in protecting cells from apoptosis by regulating the redox state of Akt.

The redox status of sulfhydryl groups is important to cellular functions such as the synthesis and folding of proteins and regulation of the structure and activity of enzymes, receptors, and transcription factors. To maintain the cellular thiol-disulfide redox status under reducing conditions, living cells possess two major systems, the thioredoxin (TRX)[1]/thioredoxin reductase system and the glutathione (GSH)/glutaredoxin (GRX) system (1).

GRX, also known as thioltransferase, was first discovered as a GSH-dependent hydrogen donor for ribonucleotide reductase in *Escherichia coli* mutants lacking TRX (2). GRX functions via a disulfide exchange reaction by utilizing the active site Cys-Pro-Tyr-Cys, which specifically and efficiently catalyzes the reduction of protein-S-S-glutathione mixed disulfide (3). Oxidized GRX is selectively recycled to the reduced form by GSH with the formation of glutathione disulfide (GSSG) and regeneration of GSH by coupling with NADPH and GSSG reductase, termed the GSH-regenerating system (4, 5). These characteristic interactions of GRX with GSH distinguish it from TRX, which favors intramolecular disulfide substrates and is turned over by NADPH and thioredoxin reductase independent of GSH. Functional overlap or cross-talk between the two systems, however, has been indicated (6, 7). GRX also partially shares its function as a redox sensor with TRX (8, 9). Although GRX has been shown to play an important role in cytoprotection against oxidative stress (10, 11) and apoptosis (12, 13), the precise mechanism of the antiapoptotic effect of GRX has not been fully elucidated.

The serine/threonine kinase Akt is a critical component of an intracellular signaling pathway that exerts effects on survival and apoptosis (14). The unphosphorylated form of Akt is virtually inactive, and phosphorylation at Thr-308 and Ser-473 stimulates its activity. Inactivation of Akt also occurs via dephosphorylation of the two phosphorylation sites by protein phosphatase 2A (PP2A) (15, 16). Akt activation contributes to the survival of hydrogen peroxide (H_2O_2)-treated cells (17). Although H_2O_2 induces the transient activation of Akt following dephosphorylation and degradation (17–19), the precise mechanism of H_2O_2-induced dephosphorylation of Akt is not well understood. Recently the crystal structure of an inactive Akt2 kinase domain has been deduced. Inactive Akt2 develops a redox-sensitive disulfide bond in its activation loop (20), which suggests that Akt is a redox-regulated protein.

Here we described a novel mechanism for the antiapoptotic effect of GRX via regulation of the redox state of Akt under oxidative stress. An intramolecular disulfide bond formed between Cys-297 and Cys-311 of Akt in cardiac H9c2 cells treated with H_2O_2. Overexpression of GRX inhibited oxidation of Akt and protected cells from apoptosis.

EXPERIMENTAL PROCEDURES

Reagents—Anti-mouse GRX antibody was affinity-purified from the serum of a rabbit immunized with a C-terminal 16-mer peptide of mouse GRX (mouse GRX-(91–106)). Anti-PP2A scaffolding A subunit (PR65) antibody was obtained from Santa Cruz Biotechnology. Anti-Akt, anti-phospho(Ser-473)-Akt, anti-phospho(Thr-308)-Akt, anti-Akt5G3, and anti-Akt1G1 antibodies were from Cell Signaling Technology. Anti-PP2A catalytic C subunit (PP2Ac) antibody was from BD Transduction Laboratories. Anti-Myc tag antibody, Akt1 cDNA Allelic Pack, and purified recombinant Akt protein (Akt/inactive and Akt/active) were from Upstate Biotechnology. c-Myc monoclonal antibody-

* This work was supported in part by grants-in-aid from the Ministry of Education, Culture, Sports, Science, and Technology, Japan. The costs of publication of this article were defrayed in part by the payment of page charges. This article must therefore be hereby marked "*advertisement*" in accordance with 18 U.S.C. Section 1734 solely to indicate this fact.

¶ To whom correspondence should be addressed. Tel.: 81-95-849-7099; Fax: 81-95-849-7100; E-mail: y-ihara@net.nagasaki-u.ac.jp.

[1] The abbreviations used are: TRX, thioredoxin; GRX, glutaredoxin; PP2A, protein phosphatase 2A; MTT, 3-(4,5-dimethyl-thiazole-2-yl)-2,5-diphenyl tetrazolium bromide; AMS, 4-acetamido-4′-maleimidylstilbene-2,2′-disulfonic acid; TUNEL, terminal deoxynucleotidyltransferase-mediated dUTP nick end labeling; LDH, lactate dehydrogenase; GSK3, glycogen synthase kinase 3; GST, glutathione *S*-transferase; myr, myristoyl; DTT, dithiothreitol; AGC, the cyclic AMP-dependent protein kinase, cyclic GMP-dependent protein kinase and protein kinase C.

agarose beads were purchased from BD Biosciences Clontech. Anti-FLAG M2 mouse monoclonal antibody, GSH, GSSG, NADPH, 3-(4,5-dimethyl-thiazole-2-yl)-2,5-diphenyl tetrazolium bromide (MTT), and L-cysteine *S*-sulfate (Cys-SO_3) were from Sigma. 4-Acetamido-4′-maleimidylstilbene-2,2′-disulfonic acid (AMS) was purchased from Molecular Probes. GSSG reductase was from Roche Applied Science. H_2O_2 and $CdCl_2$ were from Wako Pure Chemicals (Osaka, Japan).

Cell Culture—H9c2 cells, a clonal line derived from embryonic rat heart, were obtained from American Type Culture Collection (CRL-1446). H9c2 cells and gene-transfected cells were cultured in Dulbecco's modified Eagle's medium supplemented with 10% fetal calf serum in a humidified atmosphere of 95% air and 5% CO_2 at 37 °C.

Vector Construction—Full-length mouse GRX cDNA subcloned into pBluescript SK(+) was obtained as described previously (21). The mouse GRX open reading frame was amplified by PCR techniques. As the 5′-primer oligonucleotides, 5′-CGGGGATCCATGGCTCAGGAGTTTGTGAACTGC-3′, which annealed to the 5′-end of GRX cDNA and introduced a BamHI site, and as the 3′-primer oligonucleotides, 5′-CTCGAATTCTTATAACTGCAGAGCTCCAATCTG-3′ complementary to the 3′ terminus of the GRX cDNA and inserting an EcoRI site, were used. The amplified DNA fragment was digested with BamHI and EcoRI and then cloned into the pCMV-tag2B expression vector (Stratagene). GRX cDNA accompanied at the 5′-end with the FLAG sequence (5′FLAG-GRX) was digested with NotI and EcoRV and then cloned into NotI/EcoRV-cut pTRE2-Hyg (BD Biosciences Clontech) and termed pTRE2Hyg-GRX. 5′FLAG-GRX was also digested with EcoRI and XhoI and then cloned into EcoRI-XhoI-cut pGEX-6p-1 (Amersham Biosciences) and termed pGEX-GRX. The nucleotide sequences were confirmed by sequencing with an ALFexpress II system (Amersham Biosciences).

Site-directed Mutagenesis—The QuikChange XL site-directed mutagenesis kit (Stratagene) was used to make point mutations of cAkt cDNA. The following are the various primers, which were used for converting two cysteine residues (Cys-297 and Cys-311) to serine in cAkt cDNA to create mutants: sense primer oligonucleotide (5′-GACTTCGGGCTGTCCAAGGAGGGGATC-3′) and antisense primer oligonucleotide (5′-GATCCCCTCCTTGGACAGCCCGAAGTC-3′) for C297S; sense primer oligonucleotide (5′-GGGGCCAGGTACTCCGGCGTTCCGGAGAATGTCTTCATAGTGGC-3′) and antisense primer oligonucleotide (5′-GCCACTATGAAGACATTCTCCGGAACGCCGGAGTACCTGGCCCC-3′) for C311S. A double mutant (C297S/C311S) was constructed using the cAkt-C297S single mutant as a DNA template and primers for C311S. These experiments were performed according to the manufacturer's protocol. The nucleotide sequences were confirmed by sequencing with an ALFexpress II system.

Gene Transfection and Selection of Cells—Gene transfection was performed using LipofectAMINE Plus reagent (Invitrogen) according to the manufacturer's protocol. A Tet-On gene expression system (BD Biosciences Clontech) was used to establish the cell line overexpressing GRX. First, H9c2 cells were transfected with the pTet-on regulation vector. Stable transfectants were screened by culturing with 500 μg/ml G418. The cloned G418-resistant cells were then transfected with pTRE2hyg or pTRE2Hyg-GRX using the same procedure as for pTet-on. Stable transfectants were screened with 100 μg/ml hygromycin B. The cloned G418-resistant and hygromycin B-resistant cells were screened for expression of GRX. After screening, cells were cultured in Dulbecco's modified Eagle's medium with 10% fetal calf serum containing 75 μg/ml G418 and 75 μg/ml hygromycin B.

Thioltransferase Activity Assay—Thioltransferase activity was assayed as described previously (5). In brief, cell lysate or purified mouse GRX was mixed with a reaction buffer consisting of 137 mM Tris-HCl buffer (pH 8.0), 0.5 mM GSH, 1.2 units of GSSG reductase, 2.5 mM Cys-SO_3, 0.35 mM NADPH, and 1.5 mM EDTA (pH 8.0). The reaction proceeded at 30 °C, and thioltransferase activity was measured spectrophotometrically at 340 nm. The net enzymatic reaction rate was obtained by subtraction of the non-enzymatic reaction rate from the total rate.

Apoptosis Assay—Apoptosis was detected by flow cytometry with the terminal deoxynucleotidyltransferase-mediated dUTP nick end labeling (TUNEL) method using an ApopTag Plus fluorescein *in situ* apoptosis detection kit (Intergen) as described previously (16).

Immunoblot Analysis—Cultured cells were harvested and lysed for 20 min at 4 °C in lysis buffer as described previously (16). The supernatants obtained by centrifugation of the lysates at 8000 × *g* for 15 min were used in subsequent experiments. Protein concentrations were determined using a BCA assay kit (Pierce). Protein samples were electrophoresed on 10, 12.5, or 15% SDS-polyacrylamide gels under reducing conditions with the exception of thiol-modified protein samples. The proteins in the gels were transferred onto a nitrocellulose membrane. The membranes were blocked in Tris-buffered saline (10 mM Tris-HCl (pH 7.5) and 0.15 M NaCl; TBS) containing 0.05% (v/v) Tween 20 (TBST) and 5% (w/v) nonfat dry milk and then reacted with primary antibodies in TBST containing 3% (w/v) bovine serum albumin overnight with constant agitation at 4 °C. After several washes with TBST, the membranes were incubated with horseradish peroxidase-conjugated anti-IgG antibodies. Proteins in the membranes were then visualized using the enhanced chemiluminescence (ECL) detection kit (Amersham Biosciences) according to the manufacturer's instructions.

Akt Activity Assay—Akt activity was assayed using an Akt assay kit (Cell Signaling Technology) according to the manufacturer's protocol with GSK3α/β fusion protein (GSK3α/β) as a substrate. Phosphorylation of GSK3α/β was assessed by immunoblot analysis using specific antibody.

Protein Phosphatase Assay—PP2A activity was assayed spectrophotometrically using the Ser/Thr phosphatase assay kit 1 (Upstate Biotechnology) according to the manufacturer's protocol. The phosphopeptide RKpTIRR (where pT is phosphothreonine) and *p*-nitrophenyl phosphate were used as phosphatase substrates.

Cell Viability Assay—The viability of cultured cells was evaluated using MTT as described previously (22). The cells (5×10^3) were placed in 100 μl of medium/well in 96-well plates and cultured overnight. After treatment with or without H_2O_2 for a period of time, 10 μl of 0.5% MTT solution was added, and the cells were incubated for 4 h. The reaction was stopped by adding 100 μl of lysis buffer (20% SDS, 50% *N*,*N*-dimethylformamide (pH 4.7)), and then cell viability was evaluated by measuring the absorbance at 570 nm using a microplate reader.

Lactate Dehydrogenase (LDH) Release Assay—The activity of LDH released into the medium was measured with an MTX-LDH kit (Kyokuto Pharmaceutical Industrial Co., Ltd., Tokyo, Japan) according to the manufacturer's instructions. The activity of the cytoplasmic enzyme released was shown as a percentage of LDH activity in the medium over the total enzyme activity. Total enzyme activity was determined by measuring the LDH activity in the lysate of cells treated with 0.2% Tween 20, which caused complete cell death.

Determination of Redox States—The redox states of proteins were assessed by modifying free thiol with AMS (23). Briefly, after incubation with or without H_2O_2, cell lysates or proteins were treated with trichloroacetic acid at a final concentration of 7.5% to denature and precipitate the proteins as well as to avoid any subsequent redox reactions. The protein precipitates were collected by centrifugation at 12,000 × *g* for 10 min at 4 °C, washed with acetone twice, and dissolved in a buffer containing 50 mM Tris-HCl (pH 7.4), 1% SDS, and 15 mM AMS. Proteins were then separated by 10% SDS-PAGE without using any reducing agents and blotted to a nitrocellulose membrane. Proteins in the membranes were then visualized by immunoblotting as described above.

Protein Purification—FLAG-tagged mouse GRX was purified with a GST gene fusion system (Amersham Biosciences) according to the manufacturer's protocol. In brief, competent *E. coli* strain BL-21(DE3) cells were transformed with pGEX-GRX, and expression was induced by adding 1 mM isopropyl-1-thio-β-D-galactopyranoside for 3 h at 37 °C. GST-fused GRX (GST-GRX) was affinity purified from cell lysates using glutathione-Sepharose 4B, and digested with PreScission protease. The cleaved GST was removed with glutathione-Sepharose 4B.

Peroxide Quantification—Peroxide was quantified using the PeroXOquant quantitative peroxide assay (Pierce) according to the manufacturer's instructions. In brief, H_2O_2 was incubated in buffer containing components of the GSH/GRX system as indicated in Fig.7*E* at room temperature for 30 min. After a 1:10 dilution of each sample was made, 10 volumes of working reagent was added to 1 volume of diluted sample and mixed well. After incubation at room temperature for 15–20 min, the purple product composed of Fe^{3+}-xylenol orange complex was detected spectrophotometrically at 570 nm.

RESULTS

Establishment and Characterization of H9c2 Cells Overexpressing the GRX Gene—To investigate the functional effect of the overexpression of GRX on the intracellular redox state, we constructed a FLAG-tagged GRX gene expression vector and transfected rat cardiac H9c2 cells with it. The Tet-On gene expression system was utilized to obtain H9c2 cells stably overexpressing GRX. After the two-step screening of G418-resistant and hygromycin B-resistant transfectants, the expression level of GRX was characterized immunologically. We obtained three clones (H9c2-GRX22, H9c2-GRX30, and H9c2-

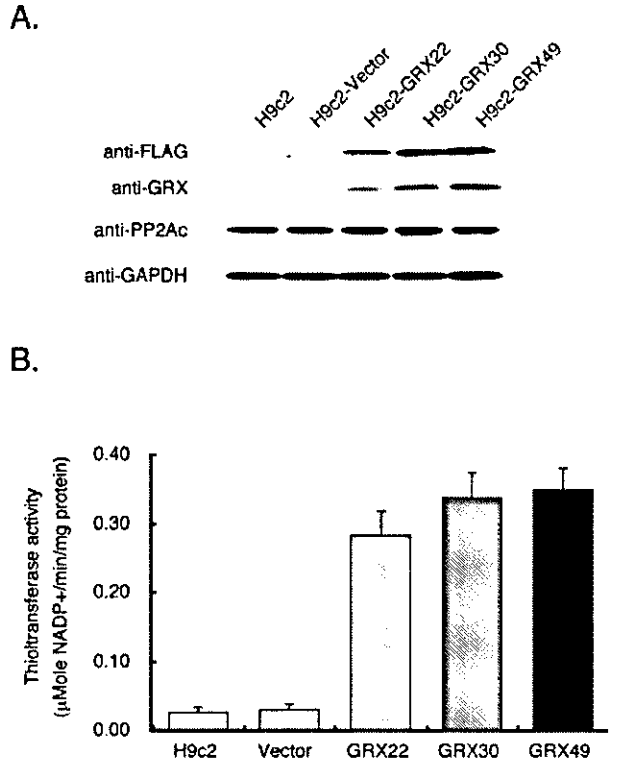

FIG. 1. **Characterization of H9c2 cells overexpressing the GRX gene.** *A*, expression of GRX in mock-transfected (*Vector*) and GRX gene-transfected H9c2 cells. The expression levels of proteins were estimated by immunoblot analysis using specific antibodies as described under "Experimental Procedures." Glyceraldehyde-3-phosphate dehydrogenase (*GAPDH*) was used to confirm that equal amounts of protein were loaded. The data represent three independent experiments. *B*, thioltransferase activity in mock-transfected (*Vector*) and GRX gene-transfected H9c2 cells was measured as described under "Experimental Procedures." The value represents the mean ± S.D. of three independent experiments.

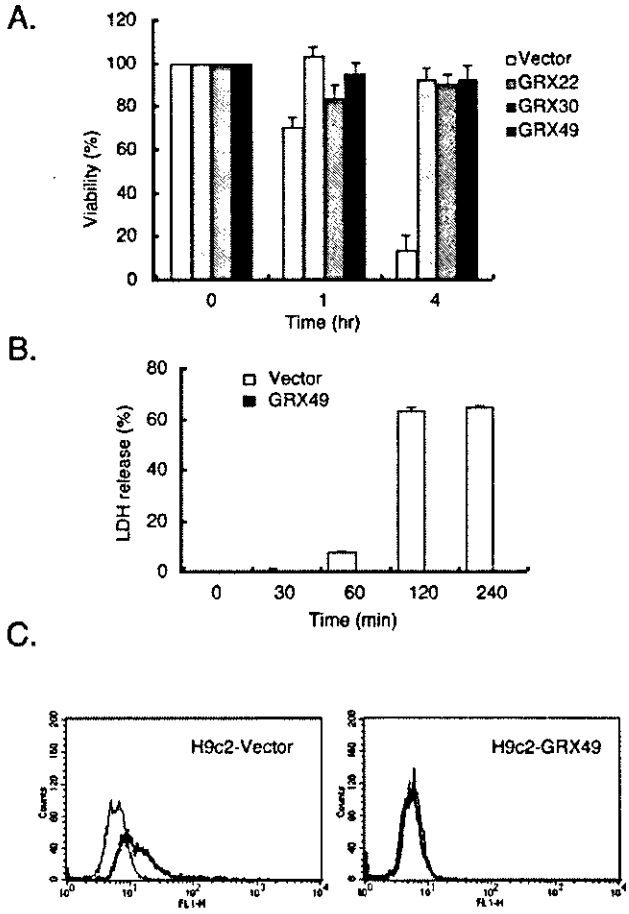

FIG. 2. **Overexpression of GRX protects H9c2 cells from H_2O_2-induced apoptosis.** Cells were treated with 100 μM H_2O_2 for the period indicated. Cell damage was assessed photometrically by the MTT assay (*A*) and LDH release assay (*B*) as described under "Experimental Procedures." *C*, apoptosis was evaluated by the TUNEL method as described under "Experimental Procedures." Cells were treated with (*thick lines*) or without (*thin lines*) 100 μM H_2O_2 for 2 h. The values in *A* and *B* represent the mean ± S.D. of three independent experiments. The data in *C* represent three independent experiments.

GRX49) that overexpressed GRX without doxycycline, so-called leaky expression (Fig. 1*A*). Although the anti-mouse GRX antibody was useful in detecting rat brain GRX immunohistochemically (24), the expression of GRX in parental and mock-transfected H9c2 cells (H9c2-Vector) was immunologically undetectable. We used no doxycycline to induce further expression of GRX in any experiments. These clones have more thioltransferase activity than parental and H9c2-Vector cells (Fig. 1*B*).

Overexpression of GRX Protects H9c2 Cells from H_2O_2-induced Apoptosis—A lower concentration (−400 μM) of H_2O_2 induces apoptosis or early mitochondrial dysfunction followed by a loss of plasma membrane integrity in H9c2 cells (25, 26). To examine the functional role of overexpressed GRX in protecting H9c2 cells against oxidative stress, mock-transfected and GRX gene-transfected H9c2 cells were treated with H_2O_2. As shown in Fig. 2*A*, the MTT assay revealed that 100 μM H_2O_2 decreased the viability of H9c2-Vector cells in a time-dependent manner but not that of GRX gene-transfected cells. In the LDH release assay, loss of plasma membrane integrity was observed in H9c2-Vector cells treated with H_2O_2 but not in H9c2-GRX49 cells (Fig. 2*B*). A TUNEL assay was carried out to clarify whether apoptosis contributed to the cell damage seen in H9c2-Vector cells treated with H_2O_2. An increase in fluorescence intensity derived from DNA strand breaks was detected in H9c2-Vector cells treated with H_2O_2 but not in H9c2-GRX49 cells (Fig. 2*C*). H9c2-GRX22 and H9c2-GRX30 cells showed results similar to H9c2-GRX49 cells in the LDH release assay and TUNEL assay (data not shown).

Involvement of Akt Signaling Pathway in the Protective Effect of GRX against H_2O_2-induced Apoptosis—The importance of the Akt signaling pathway in protecting cardiomyocytes from apoptosis has been reported (27). We investigated the phosphorylation of Akt immunologically in the cells treated with 100 μM H_2O_2. In H9c2-Vector cells, Akt activity increased to a maximum 10–30 min after the addition of H_2O_2 and then returned to basal levels by 60 min. After 120 min of treatment, Akt underwent degradation. On the other hand, a sustained phosphorylation of Akt for at least 240 min was observed without degradation in H9c2-GRX49 cells treated with H_2O_2 (Fig. 3, *A* and *B*).

To clarify the significance of the sustained activation of the Akt signaling pathway in protecting H9c2 cells from apoptosis under oxidative stress, H9c2 cells transfected with myr-Akt1-pUSEamp(+), which expresses an N-terminal myristoylated constitutively active Akt (myrAkt), were treated with 100 μM H_2O_2 for 2 h, and apoptosis was evaluated by TUNEL assay. Overexpression of myrAkt enhanced intracellular Akt kinase activity (Fig. 3, *C*, *D*, and *E*). Treatment with 100 μM H_2O_2 induced apoptosis in pUSEamp(+) vector-transfected cells (H9c2-Vector2) but not in cells overexpressing myrAkt (H9c2-myrAkt) (Fig. 3*F*).

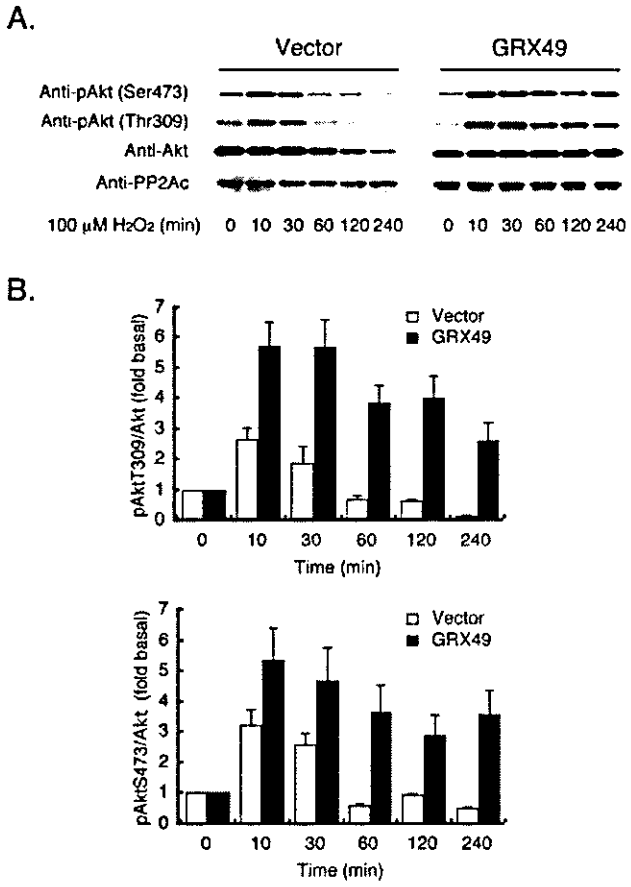

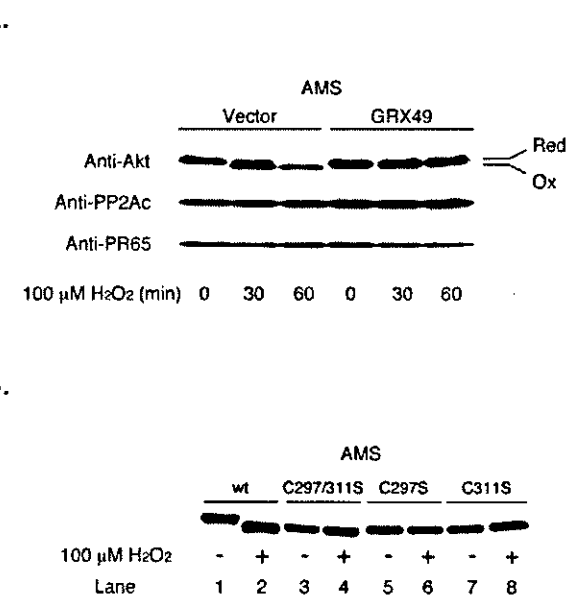

FIG. 4. **H_2O_2-induced modulation of the redox state of Akt.** *A*, cells were treated with 100 μM H_2O_2 for the period indicated. Proteins from the cells were denatured and modified with AMS as described under "Experimental Procedures." Redox states of proteins were assessed based on mobility shifts of these proteins in immunoblot analysis. The positions of reduced (*Red*) and oxidized (*Ox*) proteins are indicated. *B*, effect of mutation of indicated cysteine residues on the H_2O_2-induced mobility shift of Akt. Expression vectors for Myc-tagged wild type (*wt*) and indicated mutants of Akt were transiently transfected into H9c2-Vector cells as described under "Experimental Procedures." After 48 h, cells were treated with 100 μM H_2O_2 for 1 h. Redox states of Myc-tagged Akt were analyzed as in *A*. The data represent three independent experiments.

H_2O_2-induced Modulation of the Redox State of Akt Is Suppressed in GRX-overexpressing H9c2 Cells—Recently it has been reported that the inactive Akt2 develops a redox-sensitive intramolecular disulfide bond close to its activation loop (20). To examine the redox states of intracellular proteins including Akt under oxidative stress, we utilized the AMS alkylation method. As shown in Fig. 4*A*, Akt existed in a fully reduced form in H9c2-Vector cells, and H_2O_2 increased the amount of oxidized Akt in a time-dependent manner. Akt existed partially in the oxidized form in H9c2-GRX49 cells without oxidative stress, but H_2O_2 did not induce further oxidation of Akt. Nei-

FIG. 3. **Akt signaling pathway in the protective effect of GRX against H_2O_2-induced apoptosis.** *A*, time course of Akt phosphorylation in H9c2-Vector and H9c2-GRX49 cells under oxidative stress. Cells were treated with 100 μM H_2O_2 for the period indicated. Phosphorylation of Akt was detected by immunoblot analysis using specific antibodies as described under "Experimental Procedures." *B*, the band intensity was estimated densitometrically, and the phosphorylation rates are expressed as the relative intensity of phosphorylated Akt to total Akt (*pAkt/Akt*). *C*, pUSEamp(+) or myr-Akt1-pUSEamp(+) was introduced into H9c2 cells as described under "Experimental Procedures." After 48 h, cells were harvested, and overexpression of myrAkt in H9c2-myrAkt cells was detected by immunoblot analysis using specific antibodies as described under "Experimental Procedures." Anti-Akt antibody detected both myrAkt and endogenous Akt in H9c2-myrAkt. *D*, after 48 h of transfection of pUSEamp(+) or myr-Akt1-pUSEamp(+) as described above, Akt was immunoprecipitated (*IP*) from cell lysates with anti-Akt monoclonal antibody-conjugated and c-Myc monoclonal antibody-conjugated agarose beads. Akt activity was measured by phosphorylation of GSK3α/β as described under "Experimental Procedures." *E*, the band intensity was estimated densitometrically. *F*, apoptosis was evaluated as in Fig. 2*C*. After 48 h of transfection of pUSEamp(+) or myr-Akt1-pUSEamp(+), cells were treated with (*thick lines*) or without (*thin lines*) 100 μM H_2O_2 for 2 h. The data in *A*, *C*, *D*, and *F* represent three independent experiments. The values in *B* and *E* represent the mean ± S.D. of three independent experiments.

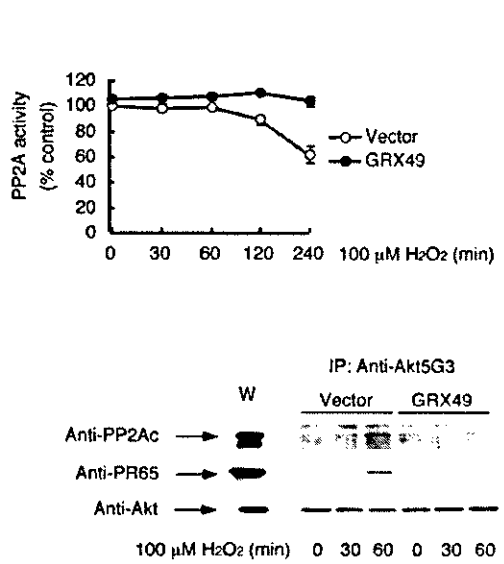

FIG. 5. **H_2O_2-induced interaction between Akt and PP2A.** *A*, PP2A activities in H9c2-Vector and H9c2-GRX49 cells treated with H_2O_2. Cells were treated with 100 μM H_2O_2 for the period indicated. PP2A activities were measured as described under "Experimental Procedures." Each value represents the mean ± S.D. of three independent experiments. *B*, interaction between Akt and PP2A in H9c2-Vector and H9c2-GRX49 cells treated with H_2O_2. Cells were treated with 100 μM H_2O_2 for the period indicated. Akt was immunoprecipitated (*IP*) from cell lysates of H9c2-Vector and H9c2-GRX49 cells with anti-Akt5G3 antibody, and the resulting immunocomplexes were subjected to immunoblot analysis using the indicated antibodies. *W* in the figure indicates whole cell lysates. The data represent three independent experiments.

ther the PP2Ac nor the PR65 underwent redox regulation by H_2O_2. Next we constructed three mutants of the Myc-tagged Akt expression vector to confirm whether the two redox-sensitive cysteines in the vicinity of the activation loop of Akt Cys-297 and Cys-311 form a disulfide bond under oxidative stress (Fig. 4*B*). H9c2-Vector cells were treated with H_2O_2 after the transfection of these vectors. Two single mutants of Akt in which a single cysteine residue was replaced with serine (C297S or C311S) showed a mobility shift between the reduced (*lane 1*) and oxidized (*lane 2*) forms of wild type Akt under non-stressful conditions (*lanes 5* and *7*). Treatment with H_2O_2 induced no mobility shift in these single mutants (*lanes 6* and *8*). The double mutant of Akt (C297S/C311S) (*lane 3*) showed almost the same mobility shift as the oxidized form of the wild type Akt (*lane 2*), and H_2O_2 did not induce a further change in mobility (*lane 4*). These results clearly demonstrated that Akt developed a disulfide bond between Cys-297 and Cys-311 in the cells under oxidative stress.

H_2O_2-induced Interaction between Akt and PP2A Is Suppressed in GRX-overexpressing H9c2 Cells—To elucidate the mechanism of the dephosphorylation of Akt after transient phosphorylation by H_2O_2, we focused on PP2A. Neither induction of PP2Ac expression (Fig. 3*A*) nor activation of PP2Ac (Fig. 5*A*) was observed in H9c2-Vector cells treated with H_2O_2. Then we examined the interaction of Akt with PP2A. As shown in Fig. 5*B*, immunoprecipitation analysis revealed that interaction between Akt and PP2A was enhanced in H9c2-Vector cells after exposure to H_2O_2 for 60 min but not in H9c2-GRX49 cells. Akt interacted at the very least with a heterodimer consisting of PP2Ac and PR65 in H9c2-Vector cells treated with H_2O_2.

Cadmium Diminished the Protective Effect of GRX on H_2O_2-induced Apoptosis—Cadmium is an inhibitor of GRX (12). Treatment with 200 μM $CdCl_2$ reduced cellular thioltransferase activity by over 60% in H9c2-GRX49 cells (Fig. 6*A*). The LDH release assay (Fig. 6*B*) and MTT assay (data not shown) revealed that treatment with 100 μM H_2O_2 in the presence of 200 μM $CdCl_2$ caused cell damage to H9c2-GRX49 cells similar to that seen with 100 μM H_2O_2 alone in H9c2-Vector cells (Fig. 2, *A* and *B*). Pretreatment with 200 μM $CdCl_2$ did not enhance the cytotoxic effect of H_2O_2 in H9c2-Vector cells (compare Fig. 6*B* to Fig. 2*B*). Treatment with H_2O_2 in the presence of $CdCl_2$ induced apoptosis in H9c2-GRX49 cells, but $CdCl_2$ alone did not (Fig. 6*C*). Cadmium also blocked the sustained activation of Akt observed in H9c2-GRX49 cells treated with H_2O_2 alone (Fig. 6, *D* and *E*). Furthermore treatment with H_2O_2 in the presence of $CdCl_2$ induced Akt oxidation in a time-dependent manner (Fig. 6*F*) and enhanced interaction between Akt and PP2A in H9c2-GRX49 cells (Fig. 6*G*). These results strongly support that GRX plays an important role in regulating the redox state of Akt under oxidative stress *in vivo*.

Redox Regulation of Akt by the GSH/GRX System in Vitro—To clarify whether the GSH/GRX system directly regulates the redox state of Akt, we examined whether GRX could protect Akt from disulfide bond formation under oxidative stress *in vitro*. First we purified mouse GRX using the GST gene fusion system (Fig. 7*A*). Purified GRX expressed thioltransferase activity (Fig. 7*B*). Then we examined the effect of purified GRX on the redox state of recombinant Akt under oxidative stress with H_2O_2. Inactive Akt existed as a fully oxidized form. On the other hand, active Akt existed as both reduced and partially oxidized forms (Fig. 7*C*). After reduction with 100 mM DTT for 1 h on ice following its removal by gel filtration, active Akt was incubated with or without 1 mM H_2O_2 under various conditions (Fig. 7*D*). H_2O_2 directly oxidized Akt independent of GSH (*lane 2*). GRX protected Akt from oxidation in a dose-dependent manner in the presence of the GSH-regenerating system (GSH/GSSG and NADPH/GSSG reductase, *lanes 10* and *12–15*). Unexpectedly GRX oxidized active Akt in GSH/GSSG buffer without H_2O_2 (*lane 5*). Yeast GRX1 and GRX2 possess glutathione peroxidase activity (28). The TRX/thioredoxin reductase and GSH/GRX systems are efficient electron donors to human plasma glutathione peroxidase, which exists where GSH levels are low (29). We also measured the peroxide scavenging activity of mouse GRX *in vitro* (Fig. 7*E*). GRX alone had the ability to reduce peroxide (*lane 9*) and worked more efficiently in the presence of the GSH/GSSG buffer (*lane 10*) or GSH-regenerating system (*lanes 11–13*). Under the same conditions as in Fig. 7*D*, *lane 15*, GRX scavenged ~60% of 1 mM H_2O_2. However, 250 μM H_2O_2 was enough to fully oxidize Akt with the GSH-regenerating system (data not shown). Taken together, mouse GRX regulates the redox state of Akt in concert with the GSH-regenerating system independent of its peroxide scavenging activity under oxidative stress.

Recombinant active Akt was reduced by incubation with DTT or oxidized by incubation with GRX in the GSH/GSSG buffer. The activity of the active form of Akt was not influenced by further reduction or oxidation (Fig. 8).

DISCUSSION

We have shown that when overexpressed GRX regulated the redox state of Akt, resulting in the protection of H9c2 cells against apoptosis under oxidative stress, and that the GSH/GRX system protected Akt from H_2O_2-induced disulfide bond formation *in vitro*. Akt existed predominantly in the reduced form in the cells not under oxidative stress. Akt developed a disulfide bond between Cys-297 and Cys-311 following treatment with H_2O_2, accompanying an increased association with PP2A. This is one possible mechanism for the transient activation of Akt following dephosphorylation under oxidative stress. Overexpression of GRX prevented Akt from developing a disulfide bond and associating with PP2A under oxidative stress.

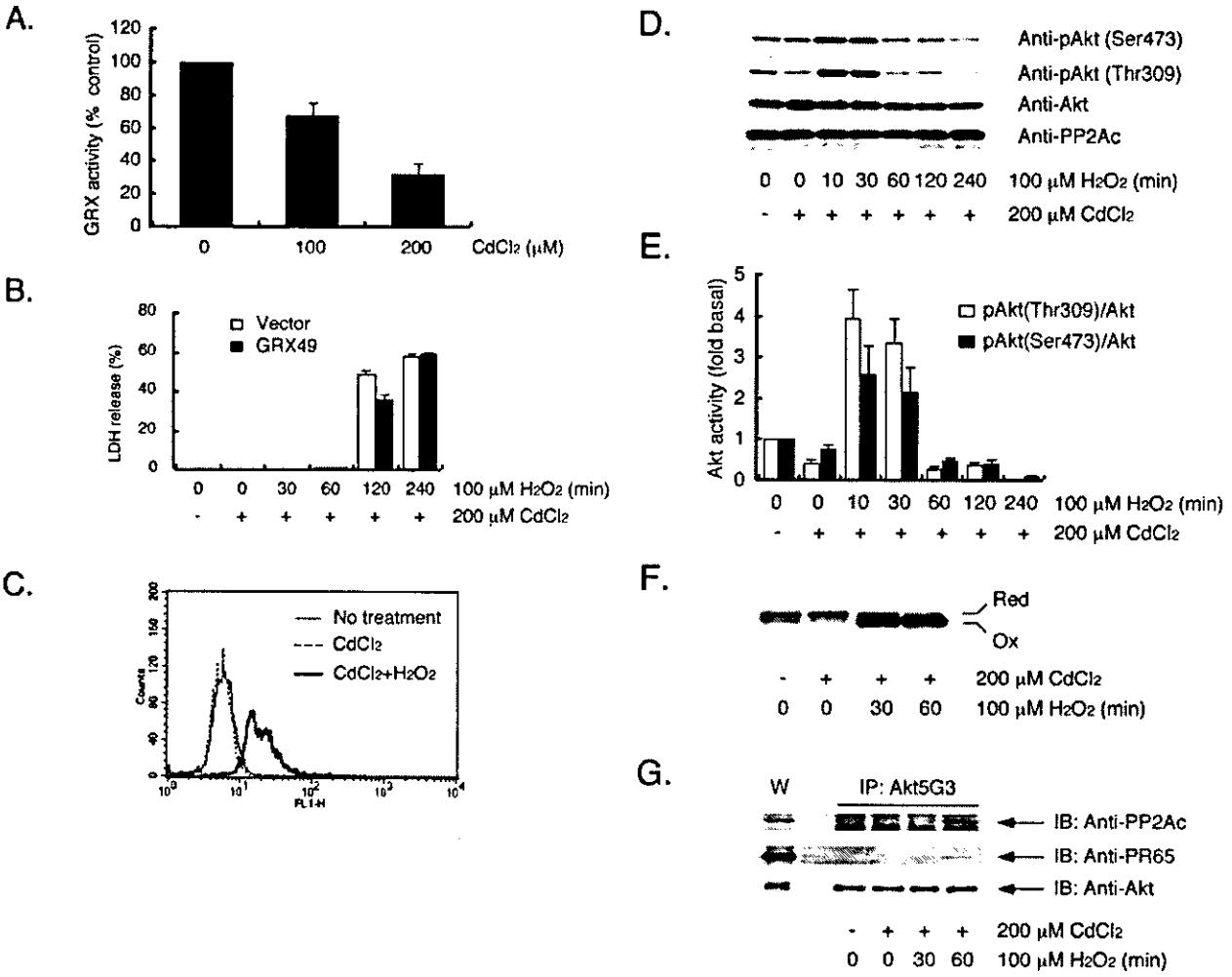

FIG. 6. **Cadmium diminished the protective effect of GRX on H_2O_2-induced apoptosis.** *A*, H9c2-GRX49 cells were treated with the indicated concentrations of $CdCl_2$ for 1 h. Thioltransferase activity was measured as described under "Experimental Procedures." *B*, H9c2-Vector and H9c2-GRX49 cells were treated with 200 μM $CdCl_2$ for 1 h prior to treatment with 100 μM H_2O_2 for the period indicated. Membrane disorder was estimated by LDH release assay as described under "Experimental Procedures." *C*, H9c2-GRX49 cells were treated with 200 μM $CdCl_2$ for 3 h (*dotted line*), with $CdCl_2$ for 1 h prior to treatment with 100 μM H_2O_2 for 2 h (*thick line*), or without any reagents (*thin line*). Apoptosis was evaluated as in Fig. 2*C*. *D*, *E*, *F*, and *G*, H9c2-GRX49 cells were treated with 200 μM $CdCl_2$ for 1 h prior to treatment with 100 μM H_2O_2 for the period indicated. *D*, time course of Akt phosphorylation in H9c2-GRX49 cells. Ser-473-phosphorylated Akt, Thr-309-phosphorylated Akt, total Akt, and PP2Ac were detected by immunoblot analysis using specific antibodies as described under "Experimental Procedures." *E*, the band intensity was estimated densitometrically, and the phosphorylation rate is expressed as in Fig. 3*B*. *F*, H_2O_2-induced mobility shift of Akt in H9c2-GRX49 cells pretreated with $CdCl_2$. The redox state of Akt was evaluated as in Fig. 4*A*. *G*, effect of $CdCl_2$ on the interaction between Akt and PP2A in H9c2-GRX49 cells treated with H_2O_2. Immunoprecipitation and immunoblotting were performed as in Fig. 5*B*. *W*, whole cell lysates. The values in *A*, *B*, and *E* represent the mean ± S.D. of three independent experiments. The data in *C*, *D*, *F*, and *G* represent three independent experiments. *pAkt*, phospho-Akt; *IB*, immunoblot; *IP*, immunoprecipitation.

The importance of the redox regulation of protein functions through the formation of an intramolecular disulfide bond has been demonstrated from *E. coli* to mammals, and both GRX and TRX are involved in this mechanism. In *E. coli*, the transcription factor OxyR is activated through intramolecular disulfide bond formation and is inactivated by enzymatic reduction with GRX1. TRX is also capable of reducing OxyR *in vitro* (30). OxyR is sensitive to oxidation and activates the expression of antioxidant genes in response to H_2O_2. The gene encoding GRX1 is regulated by OxyR (31), thus providing a mechanism for autoregulation. Likewise RsrA, an anti-σ factor in *Streptomyces coelicolor*, is regulated by redox change, and TRX reduces oxidized RsrA (32). RsrA-TRX is also suggested to create feedback homeostasis loops for its own expression. Another transcription factor and a molecular chaperone have also been shown to be activated by intramolecular disulfide bond formation (33, 34). Yap1, a functional homologue of the bacterial OxyR, regulates hydroperoxide homeostasis in *Saccharomyces cerevisiae*. Although Yap1 is activated by oxidation, it is not directly oxidized. Glutathione peroxidase 3 was identified as a second component of the pathway, serving as a sensor and transducer of the hydroperoxide signal sent to Yap1 (35). TRX turns off the pathway by reducing both sensor and regulator (35, 36). In mammalian HeLa and NIH3T3 cells, the tumor suppressor PTEN undergoes reversible intramolecular disulfide bond formation and inactivation by H_2O_2 (37), which is also one of the mechanisms of transient activation of Akt following dephosphorylation under oxidative stress. Although the best candidate for the intracellular reducing agent of oxidized PTEN was considered to be TRX, the role of the GSH/GRX system was not fully elucidated.

Transcription of GRX is regulated by an oxidative stress-induced transcription factor from *E. coli* to mammals. Recently the human GRX gene has been reported to be regulated by the

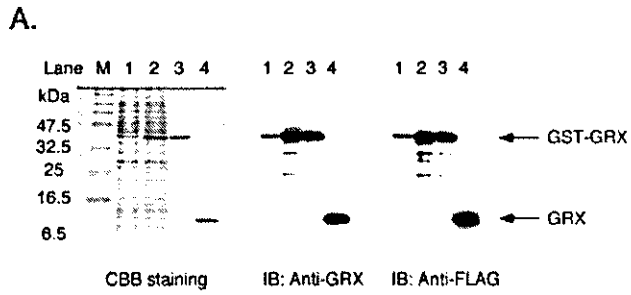

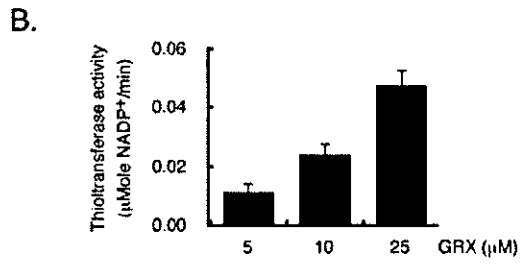

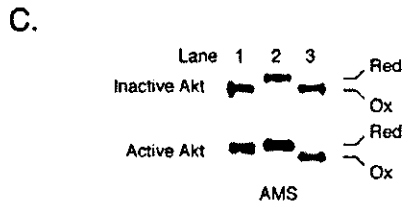

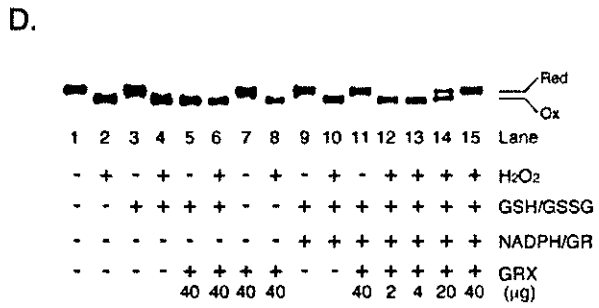

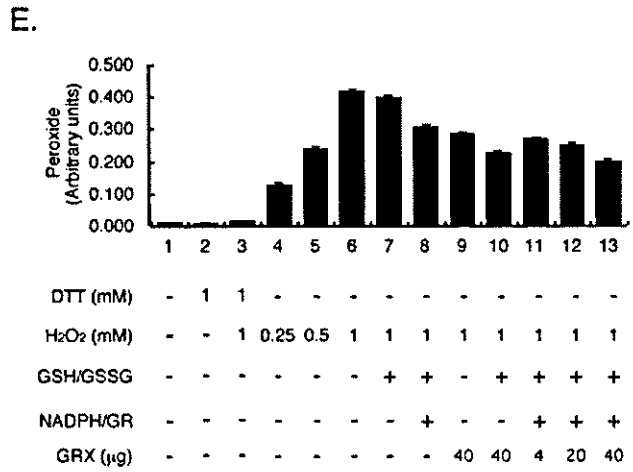

FIG. 7. **Redox regulation of Akt by the GSH/GRX system *in vitro*.** *A*, purification of GRX was analyzed by SDS-PAGE followed by Coomassie Brilliant Blue (*CBB*) staining and immunoblotting (*IB*) with antibodies against mouse GRX (*Anti-GRX*) and FLAG (*Anti-FLAG*). *M*, prestained protein marker; *lane 1*, lysates of *E. coli* BL21 cells transformed with pGEX-GRX before adding isopropyl-1-thio-β-D-galactopyranoside; *lane 2*, lysates of *E. coli* BL21 cells transformed with pGEX-GRX 3 h after adding isopropyl-1-thio-β-D-galactopyranoside; *lane 3*, GST-GRX purified with glutathione-Sepharose 4B and elution with buffer containing 10 mM reduced glutathione; *lane 4*, GRX purified by removal of cleaved GST using glutathione-Sepharose 4B following PreScission digestion. *B*, thioltransferase activity of purified mouse GRX was measured as described under "Experimental Procedures." *C*, redox state of recombinant active and inactive Akt. Recombinant active and inactive Akt were desalted by gel filtration on NAP-5 columns (Amersham Biosciences) and incubated with 100 mM DTT on ice for 1 h (*lane 2*) or with 1 mM H_2O_2 for 30 min at room temperature (*lane 3*). Samples for *lanes 2* and *3* were gel filtrated again, whereas samples for *lane 1* were immediately denatured after the first gel filtration. All samples were modified with AMS and subjected to immunoblot analysis using the anti-Akt antibody. *D*, redox state of recombinant active Akt in the presence or absence of H_2O_2 in buffer containing components of the GSH/GRX system. Recombinant active Akt was completely reduced by incubation with 100 mM DTT for 1 h on ice. DTT was then removed by gel filtration as described above. Reduced Akt (0.5 μg) was incubated with or without 1 mM H_2O_2 in buffer containing components of the GSH/GRX system as indicated in the figure at room temperature for 30 min. GSH/GSSG, 1 mM GSH and 0.05 mM GSSG; NADPH/GSSG reductase (*GR*), 1 mM NADPH and 1.2 units of GSSG reductase. The redox state of Akt was evaluated as described above. *E*, peroxides in the reaction buffer used in Fig. 7*D* were quantified as described under "Experimental Procedures." The data in *A*, *C*, and *D* represent three independent experiments. The values in *B* and *E* represent the mean ± S.D. of three independent experiments. *Red*, reduced; *Ox*, oxidized.

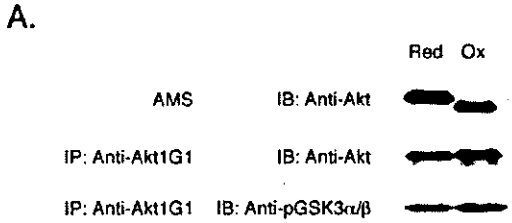

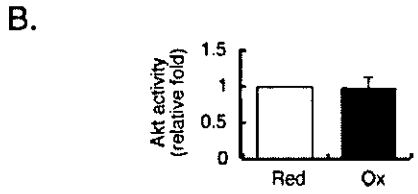

FIG. 8. **Redox state of Akt did not affect its kinase activity *in vitro*.** *A*, measurement of kinase activity of reduced or oxidized active Akt. Recombinant active Akt was incubated with 100 mM DTT on ice for 1 h or with 1 mM GSH, 0.05 mM GSSG, and 40 μg of mouse GRX at room temperature for 30 min to form reduced (*Red*) or oxidized (*Ox*) active Akt, respectively. Akt activity was measured by phosphorylation of GSK3α/β as described under "Experimental Procedures." *B*, the band intensity was estimated densitometrically, and the Akt kinase activity is expressed as the relative intensity of phosphorylated GSK3α/β/immunoprecipitated Akt. The data represent three independent experiments. *IP*, immunoprecipitation; *IB*, immunoblot; *pGSK3α/β*, phospho-GSK3α/β.

transcription factor AP-1 under oxidative stress in lens epithelial cells (38). GRX protects cerebellar granule neurons from dopamine-induced cell death by dual activation of the Ras-phosphatidylinositol 3-kinase-Akt and c-Jun N-terminal kinase pathways (13), indicating the existence of cross-talk between the two pathways. Furthermore GSK3, a substrate of Akt, negatively regulates the transcription factor AP-1 (39, 40). These findings imply the existence of an Akt-GRX autoregulation loop like OxyR-GRX1 or RsrA-TRX.

In the activation loop of the inactive Akt2 kinase domain,

Cys-297 forms a redox-sensitive disulfide bond with Cys-311 (20). Akt belongs to the so-called AGC superfamily of serine/threonine kinases. The cysteine residues identical to Cys-297 and Cys-311 of Akt are conserved in most members of the AGC superfamily, such as p70-S6K, serum- and glucocorticoid-inducible kinase, protein kinase C-related kinase 2, and protein kinase C. Several studies have reported that the AGC superfamily underwent oxidative regulation (41). Although the precise mechanisms of redox regulation of these kinases have not been elucidated, disulfide bond formation in the conserved cysteine residues would provide a possible explanation.

The effect of thiol alkylation on platelet-derived growth factor-BB-induced cell survival events has been studied (42). Platelet-derived growth factor-BB-induced Akt phosphorylation was found to be blocked by *N*-ethylmaleimide at the level of Akt, which supports our findings that Akt undergoes redox regulation. *N*-Ethylmaleimide alone or in concert with platelet-derived growth factor-BB increased PP2A activity, which depended on ceramide production following reactive oxygen species generation. In our study, no increase of PP2A activity was observed (Fig. 5*A*), but interaction between Akt and PP2A increased coinciding with Akt oxidation and dephosphorylation (Fig. 5*B*) in H9c2-Vector cells treated with H_2O_2. The redox state of Akt itself, however, did not affect the Akt activity *in vitro* (Fig. 8). These results imply the relevance of PP2A in dephosphorylation of Akt after transient phosphorylation under oxidative stress.

PP2A consists of three subunits (43). The core enzyme is a dimer, consisting of a catalytic C subunit (PP2Ac) and a scaffolding A subunit (PR65). A third regulatory B subunit can be associated with this core structure. The B subunit constitutes four different families, which can bind to the AC dimer to form a wide variety of heterotrimeric complexes. B subunits determine the substrate specificity, subcellular localization, and catalytic activity of the core enzyme. Although glutathionylation is one of the mechanisms of regulation of PP2A activity (44), PP2Ac and PR65 did not undergo redox regulation under oxidative stress (Fig. 5*A*). The regulatory B subunit specific for Akt, although unidentified, might be redox-regulated and be another key regulator of Akt dephosphorylation under oxidative stress.

In summary, GRX plays an important role in protecting cells from H_2O_2-induced apoptosis by regulating the redox state of Akt through the GSH-regenerating system. The identification of other redox-sensitive proteins regulated by GRX is crucial for understanding further the antiapoptotic functions of GRX.

Acknowledgment—We thank Noriko Sadakata for technical assistance.

REFERENCES

1. Holmgren, A. (1989) *J. Biol. Chem.* **264,** 13963–13966
2. Holmgren, A. (1976) *Proc. Natl. Acad. Sci. U. S. A.* **73,** 2275–2279
3. Gravina, S. A., and Mieyal, J. J. (1993) *Biochemistry* **32,** 3368–3376
4. Holmgren, A. (1979) *J. Biol. Chem.* **254,** 3672–3678
5. Gan, Z. R., and Wells, W. W. (1986) *J. Biol. Chem.* **261,** 996–1001
6. Prinz, W. A., Åslund, F., Holmgren, A., and Beckwith, J. (1997) *J. Biol. Chem.* **272,** 15661–15667
7. Casagrande, S., Bonetto, V., Fratelli, M., Gianazza, E., Eberini, I., Massignan, T., Salmona, M., Chang, G., Holmgren, A., and Ghezzi, P. (2002) *Proc. Natl. Acad. Sci. U. S. A.* **99,** 9745–9749
8. Song, J. J., Rhee, J. G., Suntharalingam, M., Walsh, S. A., Spitz, D. R., and Lee, Y. J. (2002) *J. Biol. Chem.* **277,** 46566–46575
9. Song, J. J., and Lee, Y. J. (2003) *Biochem. J.* **373,** 845–853
10. Luikenhuis, S., Perrone, G., Dawes, I. W., and Grant, C. M. (1998) *Mol. Biol. Cell* **9,** 1081–1091
11. Rodríguez-Manzaneque, M. T., Ros, J., Cabiscol, E., Sorribas, A., and Herrero, E. (1999) *Mol. Cell. Biol.* **19,** 8180–8190
12. Chrestensen, C. A., Starke, D. W., and Mieyal, J. J. (2000) *J. Biol. Chem.* **275,** 26556–26565
13. Daily, D., Vlamis-Gardikas, A., Offen, D., Mittelman, L., Melamed, E., Holmgren, A., and Barzilai, A. (2001) *J. Biol. Chem.* **276,** 21618–21626
14. Brazil, D. P., and Hemmings, B. A. (2001) *Trends Biochem. Sci.* **26,** 657–664
15. Andjelković, M., Jakubowicz, T., Cron, P., Ming, X. F., Han, J. W., and Hemmings, B. A. (1996) *Proc. Natl. Acad. Sci. U. S. A.* **93,** 5699–5704
16. Kageyama, K., Ihara, Y., Goto, S., Urata, Y., Toda, G., Yano, K., and Kondo, T. (2002) *J. Biol. Chem.* **277,** 19255–19264
17. Pham, F. H., Sugden, P. H., and Clerk, A. (2000) *Circ. Res.* **86,** 1252–1258
18. Ushio-Fukai, M., Alexander, R. W., Akers, M., Yin, Q., Fujio, Y., Walsh, K., and Griendling, K. K. (1999) *J. Biol. Chem.* **274,** 22699–22704
19. Martín, D., Salinas, M., Fujita, N., Tsuruo, T., and Cuadrado, A. (2002) *J. Biol. Chem.* **277,** 42943–42952
20. Huang, X., Begley, M., Morgenstern, K. A., Gu, Y., Rose, P., Zhao, H., and Zhu, X. (2003) *Structure (Camb.)* **11,** 21–30
21. Nakamura, T., Ohno, T., Hirota, K., Nishiyama, A., Nakamura, H., Wada, H., and Yodoi, J. (1999) *Free Radic. Res.* **31,** 357–365
22. Mosmann, T. (1983) *J. Immunol. Methods* **65,** 55–63
23. Kobayashi, T., Kishigami, S., Sone, M., Inokuchi, H., Mogi, T., and Ito, K. (1997) *Proc. Natl. Acad. Sci. U. S. A.* **94,** 11857–11862
24. Takagi, Y., Nakamura, T., Nishiyama, A., Nozaki, K., Tanaka, T., Hashimoto, N., and Yodoi, J. (1999) *Biochem. Biophys. Res. Commun.* **258,** 390–394
25. Turner, N. A., Xia, F., Azhar, G., Zhang, X., Liu, L., and Wei, J. Y. (1998) *J. Mol. Cell. Cardiol.* **30,** 1789–1801
26. Neuss, M., Monticone, R., Lundberg, M. S., Chesley, A. T., Fleck, E., and Crow, M. T. (2001) *J. Biol. Chem.* **276,** 33915–33922
27. Fujio, Y., Nguyen, T., Wencker, D., Kitsis, R. N., and Walsh, K. (2000) *Circulation* **101,** 660–667
28. Collinson, E. J., Wheeler, G. L., Garrido, E. O., Avery, A. M., Avery, S. V., and Grant, C. M. (2002) *J. Biol. Chem.* **277,** 16712–16717
29. Björnstedt, M., Xue, J., Huang, W., Akesson, B., and Holmgren, A. (1994) *J. Biol. Chem.* **269,** 29382–29384
30. Zheng, M., Åslund, F., and Storz, G. (1998) *Science* **279,** 1718–1721
31. Tao, K. (1997) *J. Bacteriol.* **179,** 5967–5970
32. Kang, J. G., Paget, M. S., Seok, Y. J., Hahn, M. Y., Bae, J. B., Hahn, J. S., Kleanthous, C., Buttner, M. J., and Roe, J. H. (1999) *EMBO J.* **18,** 4292–4298
33. Gostick, D. O., Green, J., Irvine, A. S., Gasson, M. J., and Guest, J. R. (1998) *Microbiology* **144,** 705–717
34. Jakob, U., Muse, W., Eser, M., and Bardwell, J. C. (1999) *Cell* **96,** 341–352
35. Delaunay, A., Pflieger, D., Barrault, M. B., Vinh, J., and Toledano, M. B. (2002) *Cell* **111,** 471–481
36. Delaunay, A., Isnard, A. D., and Toledano, M. B. (2000) *EMBO J.* **19,** 5157–5166
37. Lee, S. R., Yang, K. S., Kwon, J., Lee, C., Jeong, W., and Rhee, S. G. (2002) *J. Biol. Chem.* **277,** 20336–20342
38. Krysan, K., and Lou, M. F. (2002) *Investig. Ophthalmol. Vis. Sci.* **43,** 1876–1883
39. Nikolakaki, E., Coffer, P. J., Hemelsoet, R., Woodgett, J. R., and Defize, L. H. (1993) *Oncogene* **8,** 833–840
40. de Groot, R. P., Auwerx, J., Bourouis, M., and Sassone-Corsi, P. (1993) *Oncogene* **8,** 841–847
41. Gopalakrishna, R., and Jaken, S. (2000) *Free Radic. Biol. Med.* **28,** 1349–1361
42. Yellaturu, C. R., Bhanoori, M., Neeli, I., and Rao, G. N. (2002) *J. Biol. Chem.* **277,** 40148–40155
43. Janssens, V., and Goris, J. (2001) *Biochem. J.* **353,** 417–439
44. Rao, R. K., and Clayton, L. W. (2002) *Biochem. Biophys. Res. Commun.* **293,** 610–616

THE JOURNAL OF BIOLOGICAL CHEMISTRY
Vol. 279, No. 49, Issue of December 3, pp. 51182–51192, 2004
Printed in U.S.A.

Antiapoptotic Activity of Akt Is Down-regulated by Ca^{2+} in Myocardiac H9c2 Cells

EVIDENCE OF Ca^{2+}-DEPENDENT REGULATION OF PROTEIN PHOSPHATASE 2Ac*

Received for publication, June 28, 2004, and in revised form, September 3, 2004
Published, JBC Papers in Press, September 16, 2004, DOI 10.1074/jbc.M407225200

Chie Yasuoka‡§¶, Yoshito Ihara‡¶‖, Satoshi Ikeda§, Yoshiyuki Miyahara§, Takahito Kondo‡, and Shigeru Kohno§

From the ‡Department of Biochemistry and Molecular Biology in Disease, Atomic Bomb Disease Institute and the §Second Department of Internal Medicine, Nagasaki University Graduate School of Biomedical Sciences, Nagasaki 852-8523, Japan

Cell survival signaling of the Akt/protein kinase B pathway was influenced by a change in the cytoplasmic free calcium concentration ($[Ca^{2+}]_i$) for over 2 h via the regulation of a Ser/Thr phosphatase, protein phosphatase 2Ac (PP2Ac), in rat myocardiac H9c2 cells. Akt was down-regulated when $[Ca^{2+}]_i$ was elevated by thapsigargin, an inhibitor of the endoplasmic reticulum Ca^{2+}-ATPase, but was up-regulated when it was suppressed by 1,2-bis(*o*-aminophenoxy)ethane-*N*,*N*,*N*′,*N*′-tetraacetic acid tetra(acetoxymethyl)ester (BAPTA-AM), a cell permeable Ca^{2+} chelator. The inactivation of Akt was well correlated with the susceptibility to oxidant-induced apoptosis in H9c2 cells. To investigate the mechanism of the Ca^{2+}-dependent regulation of Akt via the regulation of PP2A, we examined the transcriptional regulation of PP2Acα in H9c2 cells with Ca^{2+} modulators. Transcription of the *PP2Acα* gene was increased by thapsigargin but decreased by BAPTA-AM. The promoter activity was examined and the cAMP response element (CRE) was found responsible for the Ca^{2+}-dependent regulation of PP2Acα. Furthermore, phosphorylation of CRE-binding protein increased with thapsigargin but decreased with BAPTA-AM. A long term change of $[Ca^{2+}]_i$ regulates *PP2Acα* gene transcription via CRE, resulting in a change in the activation status of Akt leading to an altered susceptibility to apoptosis.

Calcium (Ca^{2+}) plays a signaling role in many important cellular functions, such as fertilization, embryonic pattern formation, differentiation, proliferation, contraction, secretion, and metabolism (1). The versatility of the Ca^{2+}-signaling mechanism in terms of speed, amplitude and spatio-temporal patterning enables elevations of Ca^{2+} to regulate many processes of cell activity. Ca^{2+} exhibits cross-talk between a variety of signaling pathways (1). Ca^{2+} affects the protein kinase A pathway by regulating the metabolism of cAMP. It also activates nitric-oxide (NO) synthase to generate NO, which in turn activates the cGMP pathway through the activation of guanylyl cyclase. The Ras/mitogen-activated protein kinase (MAPK)[1] and Ca^{2+}/calmodulin/calmodulin kinase (CaMK) pathways are also controlled by Ca^{2+} (1, 2).

On the other hand, a cellular Ca^{2+} overload or the perturbation of intracellular Ca^{2+} compartmentalization can cause cytotoxicity and trigger apoptosis or necrosis (3, 4). Under such circumstances, various Ca^{2+}-dependent signaling cascades with kinases and phosphatases directly or indirectly influence cellular signaling. Protein kinase C family has been proposed to play an important role in the Ca^{2+}-mediated signaling of apoptosis (5). Calcineurin/PP2B, a Ca^{2+}-dependent Ser/Thr phosphatase (6), also appears to be involved in apoptosis (7). Together, these findings show that Ca^{2+} has a pivotal role in the regulatory mechanism of signaling pathways in cell survival and death, although the precise mechanism of Ca^{2+}-dependent cross-talk has not been fully clarified.

Akt/protein kinase B is a pleckstrin homology domain-containing Ser/Thr kinase (8, 9, 10). Akt is presently recognized as a cell survival or an antiapoptotic cellular signaling mediator. Akt is activated through a growth factor receptor-mediated activation of the phosphatidylinositol 3-kinase (PI3K) pathway (10). With growth factor signals, Akt is recruited to the plasma membrane and is activated through phosphorylation at Ser-473 and Thr-308 by phosphatidylinositol 3-phosphate-dependent protein kinase-1 (PDK1) or integrin-linked kinase (9, 10). Akt can phosphorylate Bad, caspase-9, and forkhead-related transcription factors, leading to their inactivation and to enhanced cell survival (8, 9, 10). Inhibitor of nuclear factor κB (IκB) kinase is also phosphorylated by Akt leading to an up-regulation of its activity and resulting in a promotion of the nuclear factor κB (NFκB)-mediated inhibition of apoptosis (8, 11, 12)

Akt has been found to be involved in cell death following the withdrawal of extracellular signaling factors, oxidative and osmotic stress, irradiation, treatment with drugs and ischemic stress (10). However, in spite that a variety of cellular stressors influence cells through Ca^{2+} signaling, the number of studies

* This work was supported in part by grants-in-aid from the Japanese Ministry of Education, Culture, Sports, Science, and Technology through the 21st Century COE program, and by a grant provided by the Ichiro Kanehara Foundation. The costs of publication of this article were defrayed in part by the payment of page charges. This article must therefore be hereby marked "*advertisement*" in accordance with 18 U.S.C. Section 1734 solely to indicate this fact.

The nucleotide sequence(s) reported in this paper has been submitted to the GenBank™/EBI Data Bank with accession number(s) AY749432.

¶ Both authors contributed equally to this work.

‖ To whom correspondence should be addressed: Dept. of Biochemistry and Molecular Biology in Disease, Atomic Bomb Disease Institute, Nagasaki University Graduate School of Biomedical Sciences, 1-12-4 Sakamoto, Nagasaki 852-8523, Japan. Tel.: 81-95-849-7099; Fax: 81-95-849-7100; E-mail: y-ihara@net.nagasaki-u.ac.jp.

[1] The abbreviations used are: MAPK, mitogen-activated protein kinase; BAPTA-AM, 1,2-bis (o-aminophenoxy) ethane-*N*,*N*,*N*′,*N*′-tetraacetic acid tetra (acetoxymethyl) ester; CRE, cAMP response element; CREB, CRE-binding protein; ER, endoplasmic reticulum; FITC, fluorescein isothiocyanate; PBS, phosphate-buffered saline; PI3K, phosphatidylinositol 3-kinase; LDH, lactate dehydrogenase; CaMK, calmodulin kinase; TUNEL, terminal deoxynucleotidyltransferase-mediated dUTP nick end-labeling; EMSA, electrophoretic mobility shift assay.

on Akt signaling and Ca^{2+} is limited. As for Akt, Ca^{2+}-dependent activation was reported in several studies (13, 14). On the other hand, there was a report that the activation of Akt is independent of Ca^{2+} (15). In contrast, we found that Akt was suppressed by an elevation of $[Ca^{2+}]_i$ in myocardiac H9c2 cells overexpressing the calreticulin gene (16). In the cells overexpressing calreticulin, protein phosphatase 2A (PP2A) was upregulated by Ca^{2+} to decrease the phosphorylation level of Akt, and the inactivated status of Akt was well correlated with the susceptibility to apoptosis in H9c2 cells under conditions for differentiation induced by retinoic acid. Collectively, these results suggest that the Ca^{2+}-dependent regulatory mechanism of Akt signaling may be important to a variety of apoptotic signaling mechanisms, although how has not been fully clarified.

In the present study, to investigate the mechanism of the Ca^{2+}-dependent regulation of Akt signaling, we examined the influence of a change of $[Ca^{2+}]_i$ on susceptibility to oxidative stress-induced cell injury and on the Akt signaling pathway in myocardiac H9c2 cells. We show that the Ca^{2+}-dependent regulation of *PP2Acα* gene transcription is controlled through the cAMP responsive element (CRE), resulting in a change in the activation status of Akt leading to an altered susceptibility to apoptosis.

MATERIALS AND METHODS

Antibodies and Reagents—Antibodies against Akt, phospho-Akt (Ser-473), and phospho-Akt (Thr-308), CRE-binding protein (CREB), and phospho-CREB (Ser-133) were purchased from Cell Signaling Technology (Beverly, MA). The antibody against Sp1 was purchased from Santa Cruz Biotechnology (Santa Cruz, CA). The reagents used in the study were all of high grade and from Sigma or Wako Pure Chemicals (Osaka, Japan).

Cell Culture—H9c2 cells from embryonic rat heart (16, 17) were obtained from American Type Culture Collection (CRL-1446). H9c2 cells were cultured in Dulbecco's modified Eagle's medium supplemented with 10% fetal bovine serum in a humidified atmosphere of 95% air and 5% CO_2 at 37 °C. Before reaching confluence, the cells were split, and plated at low density in culture medium containing 10% fetal bovine serum.

Measurement of Cytoplasmic Free Ca^{2+}—The cytoplasmic free Ca^{2+} concentration, $[Ca^{2+}]_i$, was measured using Fura-2-AM essentially as described previously (16). Briefly, cultured cells on glass coverslips were loaded with 5 μM Fura-2-AM (Dojindo, Kumamoto, Japan) for 20 min in Earle's balanced salt solution (EBSS) in the presence of 0.01% pluronic acid F-127. After four washes with EBSS, the cover glass was positioned in a quartz cuvette containing 3.5 ml of fresh EBSS at a 45° angle to both excitation and emission light paths. The fura-2 fluorescence was determined at 37 °C using a spectrofluorophotometer operating at an emission wavelength of 505 nm with an excitation wavelength of 340 and 380 nm. The maximal signal (R_{max}) was obtained by adding ionomycin at a final concentration of 4 μM. Then the minimal signal (R_{min}) was obtained by adding EGTA at a final concentration of 7.5 mM, followed by Tris-free base to a final concentration of 30 mM, to increase the pH to 8.3. R is the ratio (F1/F2) of the fluorescence of Ex 340 nm, Em 505 nm (F1) to that of Ex 380 nm, Em 505 nm (F2). The actual Ca^{2+} concentration was calculated as $K_d \times (R - R_{min})/(R_{max} - R)$ with the K_d equal to 224 nM (18).

Lactate Dehydrogenase (LDH) Release Assay—After 4 h of treatment with 5 μM thapsigargin or 10 μM BAPTA-AM or not, cells were incubated with 75 μM hydrogen peroxide (H_2O_2) for 0–120 min. The LDH activity was assayed by using a MTX LDH kit (Kyokuto Seiyaku, Tokyo, Japan) according to the manufacturer's instructions. Briefly, 50 μl of supernatant was transferred to a 96-well plate, then 50 μl of coloring reagent was added and incubated for 45 min at room temperature. After 100 μl of stop solution was added, absorbance was measured at 560 nm with a microplate reader. The LDH release was shown as a rate of LDH released in the medium to total cellular LDH.

TUNEL Assay—Apoptosis was detected flow cytometrically by the terminal deoxynucleotidyltransferase-mediated dUTP nick-end labeling (TUNEL) method (19) using an ApopTag Plus Fluorescein *in situ* Apoptosis Detection kit (Serologicals, Norcross, GA). Briefly, cells were harvested and fixed in 70% ethanol, treated with terminal deoxynucleotidyl transferase for 1 h, and then with fluorescein isothiocyanate (FITC)-conjugated antidigoxigenin for 1 h at room temperature, and washed with phosphate-buffered saline (pH 7.0) (PBS) containing 0.1% Triton X-100. The fluorescence intensity was measured at 530 nm using a flow cytometer (BD Biosciences, San Jose, CA).

Northern Blot Analysis—The full-length rat PP1α catalytic subunit and PP2A catalytic α cDNAs were generously provided by Dr. Kunimi Kikuchi (Hokkaido University, Japan) (20, 21). A PstI-SmaI fragment of 600 bp and EcoRI-PvuII fragment of 680 bp were prepared from the cDNAs of PP1αc and PP2Acα, respectively, and used as cDNA probes. The probes were labeled with ^{32}P using a Random Primer Labeling kit (Takara Biomedicals, Shiga, Japan). The isolation of cytoplasmic RNA and Northern blotting were essentially performed as described before (16). Isolated RNAs (10 μg) were electrophoresed on a 1% agarose gel containing 0.6 M formaldehyde, transferred to a nylon membrane, and then hybridized with ^{32}P-labeled probes. Autoradiographed membranes were analyzed using a BAS5000 bioimage analyzer (Fuji Photo Film).

Immunoblot Analysis—Cultured cells were harvested and lysed for 20 min at 4 °C in lysis buffer (20 mM Tris-HCl, pH 7.5, 130 mM NaCl, 1% Nonidet P-40, and 10% glycerol including protease inhibitors (20 μM amidinophenylmethanesulfonyl fluoride, 50 μM pepstatin, and 50 μM leupeptin)). The supernatants obtained on centrifugation at 8,000 × *g* for 10 min were used in subsequent experiments. Protein samples were subjected to 10% SDS-PAGE under reducing conditions and then transferred to nitrocellulose membrane as described (22). The membrane was blocked with 5% skim milk or 3% bovine serum albumin in Tris-buffered saline (pH 7.5) containing 0.05% Tween 20. The blots were coupled with the peroxidase-conjugated secondary antibodies, washed, and then developed using the ECL chemiluminescence delection kit (Amersham Biosciences) according to the manufacturer's instructions.

Akt Activity Assay—Akt acitivity was assayed using an Akt assay kit (Cell Signaling Technology) according to the manufacturer's protocol. Briefly, Akt was immunoprecipitated from cell lysates using the anti-Akt antibody, and then the immunoprecipitates were incubated at 30 °C for 30 min in an assay mixture containing an Akt substrate, GSK-3α/β fusion protein. Phosphorylated proteins were separated by 12.5% SDS-PAGE and then transferred to nitrocellulose membrane to detect phosphorylated GSK-3α/β using an anti-phosphorylated GSK-3α/β (Ser-21/9) antibody.

Protein Phosphatase Assay—Protein Ser/Thr phosphatase activity was assayed photometrically using Ser/Thr phosphatase assay kit 1 (Upstate Biotechnology, Lake Placid, NY), according to the manufacturer's directions. The activity was assayed in the presence or absence of 10 nM okadaic acid, and the okadaic acid-sensitive activity was estimated as PP2A-specific activity. The phosphopeptide (RK(pT)IRR) was used as a phosphatase substrate. Protein concentrations were determined using a BCA assay kit (Pierce).

Generation of Luciferase Reporter Constructs—A ~1.6-kb fragment of rat *PP2Acα* gene promoter (−1350 to +258) (23) was amplified with rat genome by PCR using *Pfu* turbo DNA polymerase (Stratagene). The primers used are as follows; a forward primer (5′-GATCTCAGGTACTTTCTTCCGGAACACTAG-3′) and a reverse primer (5′-GTCCAGCTCCTTGGTGAACAACTTC-3′). The PCR product was subcloned into pUC18 to obtain pUC18-pro-PP2Ac. The nucleotide sequence was confirmed by sequencing with an ALFexpress II system (Amersham Biosciences). pUC18-pro-PP2Ac was digested with HindIII, and the resulting fragment containing the promoter region from −1209 to +258 was inserted into the HindIII site of the reporter vector pGL3-Basic (Stratagene) to give pGL3-pro-PP2Ac. To generate deleted mutants of the luciferase reporter construct, pGL3-pro-PP2Ac was digested with SacI and XhoI, and deletion mutants were made using a deletion kit for kilo sequence (Takara Biomedicals).

Site-directed Mutagenesis for Luciferase Vectors—In vitro mutagenesis was performed with pGL3-pro-PP2Ac-del (−279 to +258) and del (−145 to +258) as templates by using a QuikChange site-directed mutagenesis kit (Stratagene). Oligonucleotides used are as follows: GC box (−155), 5′-CCCTCCCCGCGGGAGGACCACAACCCAAAAGCGAAGCCACTTCC-3′; CRE (−26), 5′-CCTGACGCCGGCGTGTGGTCACCACGCCGGGCGGCCGCCATTAC-3′. The nucleotide sequences were confirmed by sequencing with an ALFexpress II system (Amersham Biosciences).

Luciferase Activity Assay—Each vector was transfected into H9c2 cells by using Lipofectamine2000 (Invitrogen) according to the manufacturer's instructions. After 24 h of transfection, cells were treated with thapsigargin (5 μM) or BAPTA-AM (10 μM), or left untreated for the periods indicated in the text. Then luciferase activity was assayed with cellular extracts by using a dual-luciferase reporter assay system (Promega).